# Chiral Lanthanocene Derivatives Containing Two Linked Amido−Cyclopentadienyl Ligands: Heterobimetallic Structure and Lactone Polymerization Activity

Kai C. Hultzsch, Thomas P. Spaniol, and Jun Okuda*

*Institut für Anorganische Chemie und Analytische Chemie, Johannes Gutenberg-Universität Mainz, J.-J.-Becher-Weg 24, D-55099 Mainz, Germany*

*Received July 10, 1997*[⊗]

Reaction of 2 equiv of dilithium amido−cyclopentadienide $Li_2(C_5R_4SiMe_2NCH_2CH_2X)$ ($C_5R_4 = C_5Me_4$, $C_5H_3tBu$; X = OMe, $NMe_2$) with anhydrous $LnCl_3$ (Ln = Y, Lu) gave $C_2$-symmetric complexes of the type $Li[Ln(\eta^5:\eta^1\text{-}C_5R_4SiMe_2NCH_2CH_2X)_2]$ containing a heterobimetallic core. The molecular structure of $Li[Y(\eta^5:\eta^1\text{-}C_5Me_4SiMe_2NCH_2CH_2OMe)_2]$ was determined by single-crystal X-ray structural analysis, which showed it to exhibit both a pseudotetrahedral yttrium as well as a tetrahedral lithium center. In accordance with a formal 20-electron configuration at the rare earth metal center Ln, the amido-nitrogen atoms are shown to be pyramidalized. In the case of $Li[Y(\eta^5:\eta^1\text{-}C_5H_3tBuSiMe_2NCH_2CH_2X)_2]$, mixtures of the two diastereomers in relative ratios depending on the reaction time are formed. The (*R,S*)-diastereomer is the kinetic product that rearranges to the thermodynamically preferred $C_2$-symmetric (*R,R*)-diastereomer in donor solvents such as THF. The molecular structures of diastereomerically pure (*R,S*)-$Li[Y(\eta^5:\eta^1\text{-}C_5H_3tBuSiMe_2NCH_2CH_2OMe)_2]$ and (*R,R*)-$Li[Y(\eta^5:\eta^1\text{-}C_5H_3tBuSiMe_2\text{-}NCH_2CH_2NMe_2)_2]$, as determined by single-crystal X-ray structural analyses, confirm the significantly different steric congestion. All heterobimetallic complexes were shown to be active in the ring-opening polymerization of $\epsilon$-caprolactone. The poly($\epsilon$-caprolactone)s obtained are of high molecular weight ($M_n$ > 30 000) and moderate polydispersity ($M_w/M_n$ < 2.0) and are produced by the action of the nucleophilic amido-nitrogen atom.



## Introduction

There is currently considerable interest in developing structurally well-characterized organometallic complexes of rare earth metals as homogeneous polymerization catalysts.[1]

Highly efficient and controllable catalyst systems include lanthanocene hydride and hydrocarbyls of the type $[(\eta^5\text{-}C_5R_5)_2LnX]_2$ (X = H, hydrocarbyl) for ethylene[2] and α-olefin[3] polymerization, living methyl methacrylate[4] polymerization, and ring-opening lactone[4c,5] polymerization. Following the reports by McLain that lanthanide alkoxides and amides containing chelate ligands are capable of ring-opening polymerization of $\epsilon$-caprolactone and lactide,[6] a number of rare-earth-based initiators including lanthanocene derivatives $[(\eta^5\text{-}C_5R_5)_2Ln(OR')]_2$ for the synthesis of aliphatic polyesters have been recently introduced.[7] Since polylactones are increasingly becoming an important class of biodegradable and biocompatible polymers,[8] the demand for new structurally defined, tunable initiators of high efficiency and stereoselectivity is increasing.

Half-sandwich alkoxo complexes of rare earths containing a linked amido−cyclopentadienyl ligand[9−11] would be ideal candidates for structurally defined initiators for ring-opening polymerization of lactones and related monomers. Bercaw et al. demonstrated that

[⊗] Abstract published in *Advance ACS Abstracts,* October 1, 1997.

(1) Yasuda, H.; Tamai, H. *Prog. Polym. Sci.* **1993**, *18*, 1097.

(2) (a) Ballard, D. G. H.; Courtis, A.; Holton, J.; McMeeking, J.; Pearce, R. *J. Chem. Soc., Chem. Commun.* **1978**, 994. (b) Watson, P. L.; Parshall, G. W. *Acc. Chem. Res.* **1985**, *18*, 51. (c) Jeske, G.; Lauke, H.; Mauermann, H.; Swepston, P. N.; Schumann, H.; Marks, T. J. *J. Am. Chem. Soc.* **1985**, *107*, 8091. (d) Jeske, G.; Schock, L. E.; Swepston, P. N.; Schumann, H.; Marks, T. J. *J. Am. Chem. Soc.* **1985**, *107*, 8103.

(3) (a) Shapiro, P. J.; Bunel, E.; Schaefer, W. P.; Bercaw, J. E. *Organometallics* **1990**, *9*, 867. (b) Shapiro, P. J.; Cotter, W. D.; Schaefer, W. P.; Labinger, J. A.; Bercaw, J. E. *J. Am. Chem. Soc.* **1994**, *116*, 4623. (c) Coughlin, E. B.; Bercaw, J. E. *J. Am. Chem. Soc.* **1992**, *114*, 7606. (d) Mitchell, J. P.; Hajela, S.; Brookhart, S. K.; Hardcastle, K. I.; Henling, L. M.; Bercaw, J. E. *J. Am. Chem. Soc.* **1996**, *118*, 1045. (e) Schaverien, C. J. *Organometallics* **1994**, *13*, 69. (f) Yasuda, H.; Ihara, E. *Tetrahedron* **1995**, *51*, 4563. (g) Ihara, E.; Nodono, M.; Yasuda, H.; Kanehisa, N.; Kai, Y. *Macromol. Chem. Phys.* **1996**, *197*, 1909.

(4) (a) Yasuda, H.; Yamamoto, H.; Yokota, K.; Miyake, S.; Nakamura, A. *J. Am. Chem. Soc.* **1992**, *114*, 4908. (b) Yasuda, H.; Yamamoto, H.; Yamashita, M.; Yokota, K.; Nakamura, A.; Miyake, S.; Kai, Y.; Kanehisa, N. *Macromolecules* **1993**, *26*, 7134. (c) Yasuda, H.; Yamamoto, H.; Takemoto, Y.; Yamashita, M.; Yokota, K.; Miyake, S.; Nakamura, A. *Makromol. Chem., Macromol. Symp.* **1993**, *67*, 187. (d) Ihara, E.; Morimoto, M.; Yasuda, H. *Macromolecules* **1995**, *28*, 7886. (e) Jiang, T.; Shen, Q.; Lin, Y.; Jin, S. *J. Organomet. Chem.* **1993**, *450*, 121. (f) Boffa, L. S.; Novak, B. M. *Macromolecules* **1994**, *27*, 6993. (g) Giardello, M. A.; Yamamoto, Y.; Brard, L.; Marks, T. J. *J. Am. Chem. Soc.* **1995**, *117*, 3276.

(5) (a) Yasuda, H.; Furo, M.; Yamamoto, H.; Nakamura, A.; Miyake, S.; Kibino, N. *Macromolecules* **1992**, *25*, 5115. (b) Yamashita, M.; Takemoto, Y.; Ihara, E.; Yasuda, H. *Macromolecules* **1996**, *29*, 1798. (c) Evans, W. J.; Katsumata, H. *Macromolecules* **1994**, *27*, 2330. (d) Evans, W. J.; Katsumata, H. *Macromolecules* **1994**, *27*, 4011.

(6) (a) McLain, S. J.; Drysdale, N. E. *Polym. Prepr. (Am. Chem. Soc., Div. Polym. Chem.)* **1992**, *33*, 174. (b) McLain, S. J.; Ford, T. M.; Drysdale, N. E. *Polym. Prepr. (Am. Chem. Soc., Div. Polym. Chem.)* **1992**, *33*, 463.

(7) (a) Le Borgne, A.; Pluta, C.; Spassky, N. *Macromol. Rapid Commun.* **1994**, *15*, 955. (b) Stevels, W. M.; Ankoné, M. J. K.; Dijkstra, P. J.; Feijen, J. *Macromol. Chem. Phys.* **1995**, *196*, 1153. (c) Stevels, W. M.; Ankoné, M. J. K.; Dijkstra, P. J.; Feijen, J. *Macromolecules* **1996**, *29*, 3332. (d) Shen, Y.; Shen, Z.; Shen, J.; Zhang, Y.; Yao, K. *Macromolecules* **1996**, *29*, 3441. (e) Shen, Y.; Shen, Z.; Zhang, Y.; Yao, K. *Macromolecules* **1996**, *29*, 8289.

(8) (a) Pierre, T. St.; Chiellini, E. *J. Bioact. Compat. Polym.* **1987**, *2*, 4. (b) Müller, H.-M.; Seebach, D. *Angew. Chem., Int. Ed. Engl.* **1993**, *32*, 477.

S0276-7333(97)00586-4 CCC: $14.00 

the 12-electron scandium hydride and alkyl complexes of the type Sc($\eta^5$:$\eta^1$-$C_5Me_4SiMe_2NCMe_3$)X (X = H, $CH_2CH_2CH_3$) function as the active α-olefin polymerization catalysts.[3a,b] Thus, an alkoxo or amido complex in this series (X = OR, $NR_2$) appeared to be a viable initiator for lactones. Because of the notoriously high Lewis-acidity of mono(cyclopentadienyl) lanthanide complexes,[12] we thought that a tridentate variant of the linked amido−cyclopentadienyl ligand [$C_5R_4SiMe_2NCH_2CH_2X$] ($C_5R_4$ = $C_5Me_4$, $C_5H_3tBu$; X = OMe, $NMe_2$)[13] containing an additional donor site would be best suited. Our attempts to prepare such species, however, led to the unexpected isolation of bis(ligand) complexes of the type Li[Ln($\eta^5$:$\eta^1$-$C_5R_4SiMe_2NCH_2CH_2X)_2$] (Ln = Y, Lu). Formally, the electronically "oversaturated" metallocene unit [Ln($\eta^5$:$\eta^1$-$C_5R_4SiMe_2NCH_2CH_2X)_2$]$^-$ incorporates two $\pi$-donating amido ligands and can be assumed to show nucleophilic behavior toward the ester carbon center. Yet at the same time, this bis(ligand) complex contains two Lewis-acidic centers in close proximity. Here we report the synthesis, characterization, and reactivity of this new class of chiral heterobimetallic complexes.

## Results and Discussion

**Synthesis and Characterization.** Attempts to synthesize mono(ligand) yttrium complexes via amine elimination from Y{$N(SiMe_3)_2$}$_3$[11] and ($C_5Me_4H$)-$SiMe_2(NHCH_2CH_2X)$ failed due to decomposition of the free ligand, possibly due to the forcing reaction conditions (110 °C in toluene, 4 days) applied. Also, reaction of $YCl_3(THF)_{3.5}$ with 1 equiv of $Li_2(C_5Me_4SiMe_2NCH_2CH_2OMe)$ in toluene or THF resulted in complex mixtures of inseparable products. However, reaction of anhydrous $YCl_3$ with 2 equiv of $Li_2(C_5Me_4SiMe_2NCH_2CH_2X)$ (X = OMe (**a**), $NMe_2$ (**b**)) in THF afforded the novel bis(ligand) yttrium complexes **1** in good yields as colorless to slightly yellow crystals (Scheme 1). Similarly, the reaction of anhydrous $LuCl_3$ with 2 equiv of $Li_2(C_5Me_4SiMe_2NCH_2CH_2OMe)$ in THF gave complex **2a** in good yield as off-white crystals. Complexes **1** and **2a** are very air- and moisture-sensitive, showing good solubility in THF and aromatic solvents, but low solubility in aliphatic hydrocarbons. They were completely characterized by elemental analysis and NMR spectroscopy. The elemental analyses were consistent with the unsolvated composition, suggesting a heterobimetallic monomeric structure containing both yttrium and lithium (Figure 1).

A single-crystal X-ray structural analysis of Li[Y($\eta^5$:$\eta^1$-$C_5Me_4SiMe_2NCH_2CH_2OMe)_2$] (**1a**) confirmed this remarkable bent metallocene structure with $C_2$-symmetry (*vide infra*). As a top view of the molecule shows, the metallocene unit basically forms an "open" $N_2O_2$-macrocycle. The coordination around the lithium atom is tetrahedral, with the side chain being distorted in a helical way. $^1$H NMR spectra of **1a**, **1b**, and **2a** in $C_6D_6$ indicated the absence of THF coordinated at the metal centers. Consistent with the chiral structure, the $^1$H NMR spectrum of **2a** at room temperature shows four signals for the methyl protons of the cyclopentadienyl ring and two signals for the methyl protons on the silicon atom (Figure 2). The four protons in each of the $CH_2CH_2$ links are diastereotopic and give rise to a complicated ABCD coupling pattern, unequivocally as-

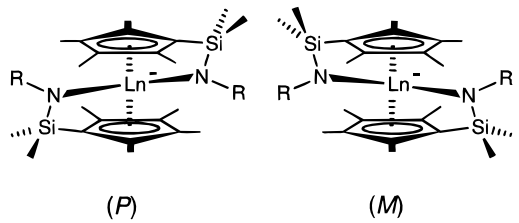


**Figure 1.** Possible enantiomeric forms of complexes **1** and **2a**. The lithium atom has been omitted for the sake of clarity (Ln = Y, Lu; R = $CH_2CH_2OMe$, $CH_2CH_2NMe_2$).

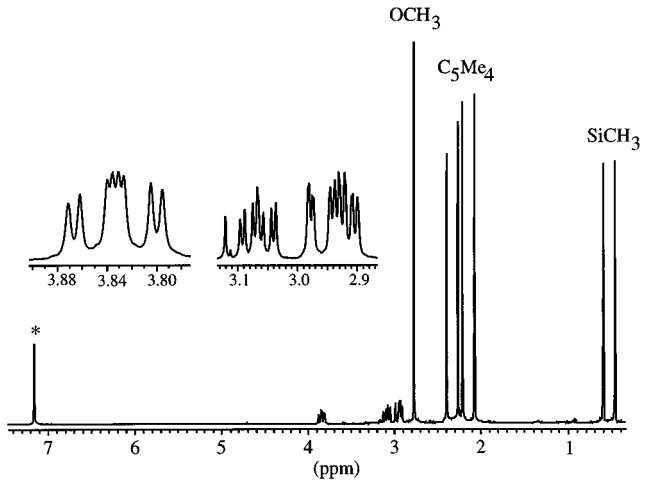


**Figure 2.** $^1$H NMR spectrum of **2a** in $C_6D_6$ at 25 °C.

**Scheme 1**

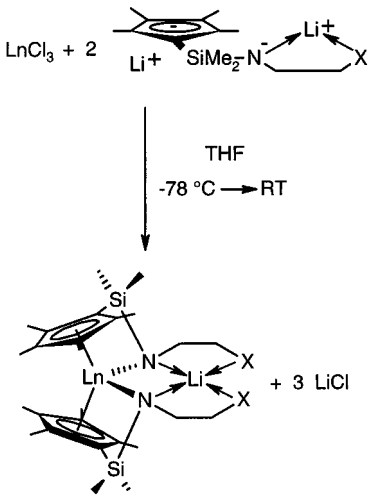


**1a** Ln = Y; X = OMe; 82 %
**1b** Ln = Y; X = $NMe_2$; 74 %
**2a** Ln = Lu; X = OMe; 82 %

(9) Mono(cyclopentadienyl) titanium alkoxides initate the ring-opening polymerization of ϵ-caprolactone, see: (a) Okuda, J.; Rushkin, I. L. *Macromolecules* **1993**, *26*, 5530. (b) Okuda, J.; Kleinhenn, T.; König, P.; Taden, I.; Ngo, S.; Rushkin, I. L. *Macromol. Symp.* **1995**, *95*, 195.

(10) (a) For a brief review on chelating cyclopentadienyl ligands in general, see: Okuda, J. *Comments Inorg. Chem.* **1994**, *16*, 185. (b) For a review on intramolecular coordinating ligands in group 3 and lanthanide chemistry, see: Hogerheide, M. P.; Boersma, J.; van Koten, G. *Coord. Chem. Rev.* **1996**, *155*, 87.

(11) Mu, Y.; Piers, W. E.; MacDonald, M.-A.; Zaworotko, M. J. *Can. J. Chem.* **1995**, *73*, 2233.

(12) (a) Schaverien, C. J. *Adv. Organomet. Chem.* **1994**, *36*, 283. (b) Edelmann, F. T. In *Comprehensive Organometallic Chemistry II*; Abel, E. W., Stone, F. G. A., Wilkinson, G., Eds.; Pergamon Press: Oxford, 1995; Vol. 4, Chapter 2. (c) Piers, W. E.; Shapiro, P. J.; Bunel, E. E.; Bercaw, J. E. *Synlett* **1990**, 74.

(13) du Plooy, K. E.; Moll, U.; Wocadlo, S.; Massa, W.; Okuda, J. *Organometallics* **1995**, *14*, 3129.

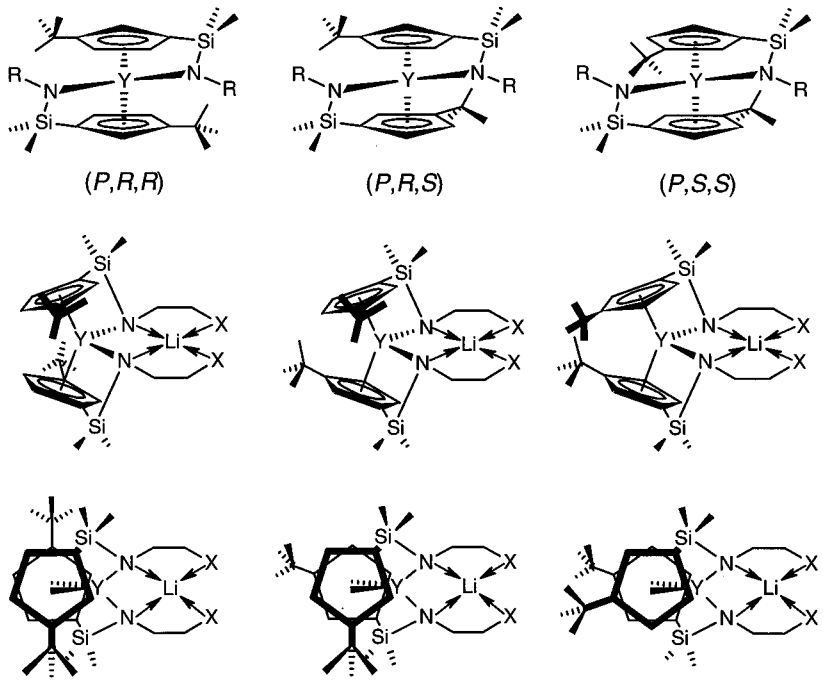


**Figure 3.** Possible diastereomers of **3**. The lithium atom has been omitted for the sake of clarity (R = $CH_2CH_2OMe$, $CH_2CH_2NMe_2$).



signed to each of the four protons of the side chain by $^1H-^{13}C$ COSY. The $^1H$ NMR spectra show one signal for the methoxy and dimethylamino groups, which are shifted to higher field as compared with those in the free ligand or in the mono(ligand) titanium and zirconium complexes of the type $M(\eta^5:\eta^1\text{-}C_5R_4SiMe_2NCH_2CH_2X)Cl_2$.[13]

Preferred formation of a bis- over a mono(ligand) complex can be ascribed to the greater ionic radius of yttrium as compared with that of scandium (1.019 vs 0.870 Å).[14] This preference for $C_2$-symmetric bis(ligand) complexes of the type $M(\eta^5:\eta^1\text{-}C_5R_4SiMe_2NR')_2$ (M = Ti, Zr; R = H, Me; R′ = $CMe_3$, $CH_2CH_2OMe$, $CH_2CH_2NMe_2$, $CH_2CH{=}CH_2$) has been previously observed in group 4 chemistry.[13,15,16] Several chiral donor-functionalized metallocene complexes of lanthanides and few group 4 metals with amine,[17] ether,[17e,18] or alkoxo[19] donors have been reported in the literature. The heterobimetallic complex $Li[Cp_2Y(NMeCH_2CH_2NMe_2)_2]$,[20] mentioned by Schumann, presumably adopts a structure similar to that of **1b**.

When the $^1H$ and $^{13}C$ NMR spectra of **1a** were recorded upon addition of 1 equiv of 12-crown-4, known to coordinate lithium ions,[21] no significant change was observed. We conclude that the lithium ion remains coordinated at the side chains of the ligand, although a fast equilibrium of the lithium ion between **1a** and 12-crown-4 on the NMR time scale cannot be excluded.

When an analogous synthesis is carried out with the ligand derived from the planar chiral 3-*tert*-butylcyclopentadienyl moiety instead of that derived from the achiral tetramethylcyclopentadienyl unit, the formation of potentially four different pairs of diastereomeric metallocenes is conceivable.[22] However, due to the *meso* relationship of the two chiral planes with respect to each other in **(*R*,*S*)-3** and **(*S*,*R*)-3**, only three diastereomers exist (Figure 3).

The reaction of anhydrous $YCl_3$ with 2 equiv of $Li_2(C_5H_3tBuSiMe_2NCH_2CH_2X)$ (X = OMe (**a**), $NMe_2$ (**b**)) in THF afforded a mixture of two diastereomeric bis(ligand) yttrium complexes **3** with (*R*,*R*) and (*R*,*S*) configurations in moderate to good yields as colorless crystals (Scheme 2). The mixture does not contain any significant amount (>5% by $^1H$ NMR spectroscopy) of the (*S*,*S*)-diastereomer. The (*R*,*S*)- and (*R*,*R*)-diastereomers can be easily distinguished by their symmetry: The $C_2$-symmetric (*R*,*R*)-diastereomer gives rise to three signals for the protons of the cyclopentadienyl rings in the $^1H$ NMR spectrum, whereas the $C_1$-symmetric (*R*,*S*)-

(14) Shannon, R. D. *Acta Crystallogr.* **1976**, *A32*, 751.
(15) Böhme, U.; Thiele, K.-H. *J. Organomet. Chem.* **1994**, *472*, 39.
(16) Herrmann, W. A.; Morawietz, M. J. A.; Priermeier, T. *Angew. Chem., Int. Ed. Engl.* **1994**, *33*, 1946.
(17) (a) Herrmann, W. A.; Anwander, R.; Munck, F. C.; Scherer, W. *Chem. Ber.* **1993**, *126*, 331. (b) Anwander, R.; Herrmann, W. A.; Scherer, W.; Munck, F. C. *J. Organomet. Chem.* **1993**, *462*, 163. (c) Jutzi, P.; Dahlhaus, J.; Kristen, M. O. *J. Organomet. Chem.* **1993**, *450*, C1. (d) van den Hende, J. R.; Hitchcock, P. B.; Lappert, M. F.; Nile, T. A. *J. Organomet. Chem.* **1994**, *472*, 79. (e) Molander, G. A.; Schumann, H.; Rosenthal, E. C. E.; Demtschuk, J. *Organometallics* **1996**, *15*, 3817.
(18) (a) Laske, D. A.; Duchateau, R.; Teuben, J. H.; Spek, A. L. *J. Organomet. Chem.* **1993**, *462*, 149. (b) Deng, D.; Li, B.; Qian, C. *Polyhedron* **1990**, *9*, 1453. (c) Deng, D.; Qian, C.; Wu, G.; Zheng, P. *J. Chem. Soc., Chem. Commun.* **1990**, 880. (d) Qian, C.; Wang, B.; Deng, D.; Wu, G.; Zheng, P. *J. Organomet. Chem.* **1992**, *427*, C29. (e) Deng, D.; Song, F.; Wang, Z.; Qian, C.; Wu, G.; Zheng, P. *Polyhedron* **1992**, *11*, 2883. (f) Deng, D.; Qian, C.; Song, F.; Wang, Z.; Wu, G.; Zheng, P. *J. Organomet. Chem.* **1993**, *443*, 79. (g) Deng, D.; Qian, C.; Song, F.; Wang, Z.; Wu, G.; Zheng, P.; Jin, S.; Lin, Y. *J. Organomet. Chem.* **1993**, *458*, 83. (h) Deng, D.; Zheng, X.; Qian, C.; Sun, J.; Zhang, L. *J. Organomet. Chem.* **1994**, *466*, 95. (i) Qian, C.; Zheng, X.; Wang, B.; Deng, D.; Sun, J. *J. Organomet. Chem.* **1994**, *466*, 101. (j) Deng, D.; Jiang, Y.; Qian, C.; Wu, G.; Zheng, P. *J. Organomet. Chem.* **1994**, *470*, 99. (k) Van de Weghe, P.; Bied, C.; Collin, J.; Marçalo, J.; Santos, I. *J. Organomet. Chem.* **1994**, *475*, 121. (l) Deng, D.; Zheng, X.; Qian, C.; Sun, J.; Dormond, A.; Baudry, D.; Visseaux, M. *J. Chem. Soc., Dalton Trans.* **1994**, 1665. (m) Qian, C.; Wang, B.; Deng, D.; Hu, J.; Chen, J.; Wu, G.; Zheng, P. *Inorg. Chem.* **1994**, *33*, 3382. (n) Trifonov, A. A.; Van de Weghe, P.; Collin, J.; Domingos, A.; Santos, I. *J. Organomet. Chem.* **1997**, *527*, 225.
(19) Christoffers, J.; Bergman, R. G. *Angew. Chem., Int. Ed. Engl.* **1995**, *34*, 2266.
(20) Schumann, H.; Lee, P. R.; Loebel, J. *Chem. Ber.* **1989**, *122*, 1897.
(21) Weber, E.; Vögtle, F. *Top. Curr. Chem.* **1981**, *98*, 1.
(22) The stereochemistry of metallocenes has been reviewed, see: Schlögl, K. *Top. Stereochem.* **1967**, *1*, 39.

**Scheme 2**

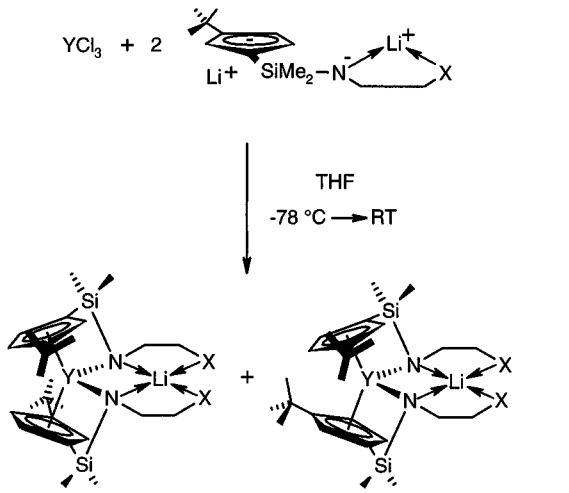


| | (*R*,*R*) | (*R*,*S*) | reaction time, h |
|---|---|---|---|
| | 1 | 16 | 3 |
| **3a** X = OMe | 1 | 6 | 6 |
| | 1.8 | 1 | 17 |
| | 1 | 5 | 3 |
| **3b** X = $NMe_2$ | 1 | 2 | 6 |
| | 3.5 | 1 | 20 |

diastereomer should show six signals. The 400 MHz $^1$H NMR spectrum of the (*R*,*S*)-diastereomer of **3a** in $C_6D_6$ shows five signals with the relative intensity of 1:1:2:1:1 due to coincidental overlap of two resonances.[23] The $^1$H NMR spectrum of the (*R*,*S*)-diastereomer of **3b** shows four signals with the relative intensity of 1:1:3:1. In addition, the $^1$H NMR spectrum of the $C_1$-symmetric (*R*,*S*)-diastereomer exhibits four $SiCH_3$ resonances and two $C(CH_3)_3$ resonances, while that of the $C_2$-symmetric (*R*,*R*)-diastereomer contains only two $SiCH_3$ resonances and one $C(CH_3)_3$ resonance. Unequivocal evidence for the identity of the two diastereomers was furnished by a single-crystal X-ray structural analysis of (*R*,*S*)-Li[Y($\eta^5$:$\eta^1$-$C_5H_3t$BuSiMe$_2$NCH$_2$CH$_2$OMe)$_2$] (**(*R*,*S*)-3a**) and (*R*,*R*)-Li[Y($\eta^5$:$\eta^1$-$C_5H_3t$BuSiMe$_2$NCH$_2$CH$_2$NMe$_2$)$_2$] (**(*R*,*R*)-3b**), which confirmed the assignment of the above NMR data. In the case of the related zirconium complex [Zr($\eta^5$:$\eta^1$-$C_5H_3t$BuCH$_2$CH$_2$O)$_2$], only the least constrained $C_2$-symmetric diastereomer with an (*R*,*R*)-configuration (both enantiomers) was formed.[19]

The relative ratio of the two diastereomers strongly depends on the reaction time. Examination of the crude reaction mixture by $^1$H NMR spectroscopy revealed that the (*R*,*S*)-diastereomer is predominant at the beginning of the reaction, whereas the (*R*,*R*)-diastereomer forms only after prolonged reaction time (Scheme 2). Therefore, it was hypothesized that the (*R*,*S*)-diastereomer forms under kinetic control while the sterically less hindered (*R*,*R*)-diastereomer is the thermodynamic product. The initially preferred formation of the (*R*,*S*)-diastereomer can be explained by the decreased sterical interaction of the *tert*-butyl substituent of the incoming cyclopentadienyl ligand from the *si* side with ligands already coordinated at yttrium.[24] Another possibility

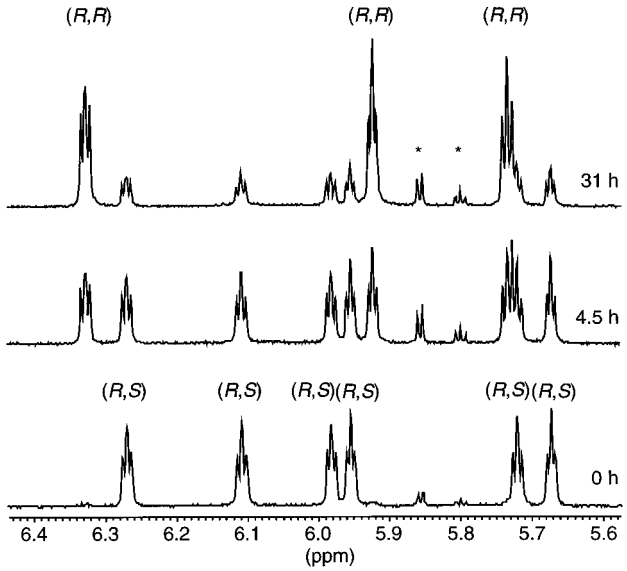


**Figure 4.** Time evolution of the cyclopentadienyl proton region of the $^1$H NMR spectrum for the epimerization of **(*R*,*S*)-3a** in THF-$d_8$ at 21 °C. The signals marked with an asterisk are due to an impurity.

would be the preferred formation of a mono(ligand) intermediate containing the planar chiral *tert*-butylcyclopentadienyl ligand with an (*S*)-configuration. The second cyclopentadienyl ligand must have an (*R*)-configuration due to sterical hindrance.

The isolated complexes are configurationally stable at room temperature in apolar solvents like benzene. However, slow epimerization occurs in donor solvents such as THF, shifting the ratio of the two diastereomers toward the thermodynamically preferred (*R*,*R*)-diastereomer. As an example, the epimerization of pure **(*R*,*S*)-3a** was examined in THF-$d_8$ by $^1$H NMR spectroscopy (Figure 4). Slow evolution of the (*R*,*R*)-diastereomer and slow decrease of the signals due to the (*R*,*S*)-diastereomer was observed, giving a final ratio of (*R*,*R*):(*R*,*S*) of 64:36 after 31 h of equilibration. Integration of the proton signals of the cyclopentadienyl region assignable to the (*R*,*S*)- and (*R*,*R*)-diastereomer revealed a first-order rate law for the approach to equilibrium (Figure 5).[26a] The forward rate constant at 21 °C was $k_1 = 2.98(5) \times 10^{-5}$ s$^{-1}$ ($t_{1/2} = 6.5$ h).[26b]

The temperature dependence of the rate constant for the epimerization of **(*R*,*S*)-3a** gave $\Delta H^{\ddagger} = 71(6)$ kJ mol$^{-1}$ and $\Delta S^{\ddagger} = -89(20)$ J K$^{-1}$ mol$^{-1}$ (Figure 6). The strong negative activation entropy is in accordance with a highly ordered transition state. The positive value of $\Delta H^{\ddagger}$ reflects the bond disruption energy required to overcome the formal charge separation between the cyclopentadienyl groups and the metal core.

This epimerization proceeds through a dissociation of one of the cyclopentadienyl ligands from the yttrium, rotation about the silicon−ring carbon bond, and recoordination of the cyclopentadienyl ligand from the

(23) One signal of a ring proton of the (*R*,*S*)-diastereomer overlaps with a signal of the (*R*,*R*)-diastereomer. The $^1$H NMR spectrum of **(*R*,*S*)-3a** in THF-$d_8$ shows six distinct signals for the protons of the cyclopentadienyl rings.

(24) Brintzinger et al. proposed the formation of an $\eta^1$-bound cyclopentadienyl intermediate during the synthesis of *rac*- and *meso-ansa*-metallocenes, see ref 25.

(25) Wiesenfeldt, H.; Reinmuth, A.; Barsties, E.; Evertz, K.; Brintzinger, H.-H. *J. Organomet. Chem.* **1989**, *369*, 359.

(26) (a) Huisgen, R. In *Houben-Weyl, Methods of Organic Chemistry*; Müller, E., Ed.; Georg Thieme Verlag: Stuttgart, 1955; Vol. III, Part 1. (b) Initial experiments suggest an increased forward rate constant in the presence of LiCl, e.g., $k_1 = 6.9(3) \times 10^{-5}$ s$^{-1}$ with 3 equiv of LiCl at 21 °C.

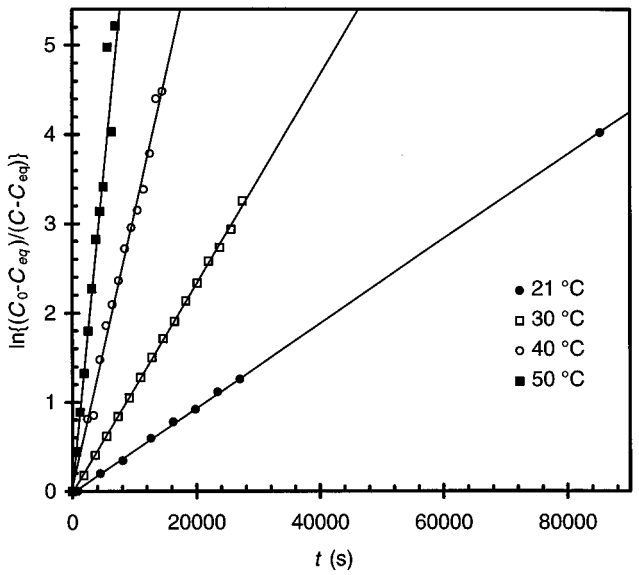


**Figure 5.** Kinetic plot for the epimerization of **(*R*,*S*)-3a** in THF-$d_8$ at different temperatures.

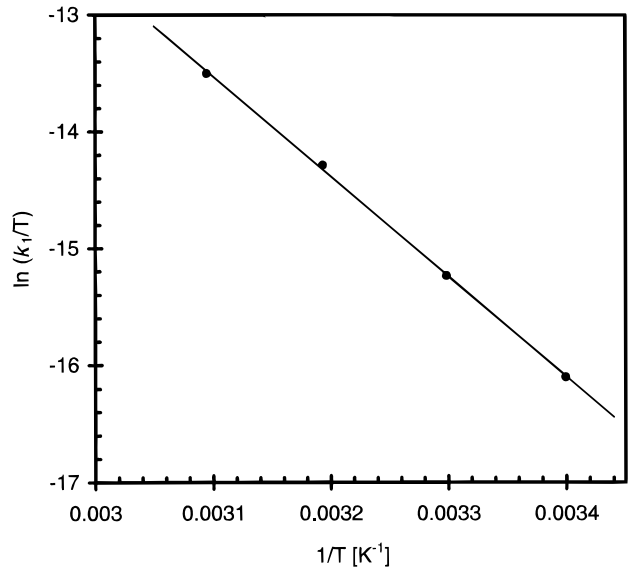


**Figure 6.** Eyring plot for the epimerization of **(*R*,*S*)-3a** in THF-$d_8$.

opposite diastereoface (Scheme 3).[27] Under the participation of donor solvent molecules, an intermediate is invoked in which the lithium induces the formation of a lithium cyclopentadienyl ion pair and in which the yttrium is coordinatively saturated by the solvents. Recently, Marks et al. observed epimerization in donor solvents of chiral $C_1$-symmetric lanthanocene complexes of the general type ($\eta^5$:$\eta^5$-$C_5Me_4SiMe_2C_5H_3R^*$)Ln($\mu$-Cl)$_2$-Li($OEt_2$)$_2$ containing an optically active substituent R*.[28] Similar isomerization was also observed during the

**Scheme 3**

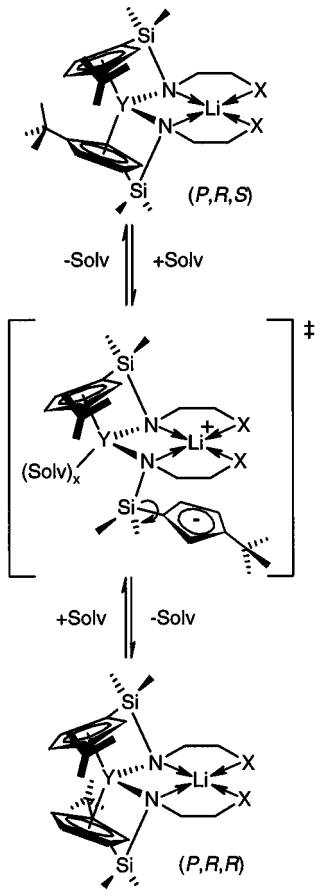


synthesis of *ansa*-zirconocenes by the amine elimination method. Here, the *meso*- and *rac*-isomers can be converted into each other under the catalytic action of $NMe_2H$.[29−31]

**Molecular Structure of Li[Y($\eta^5$:$\eta^1$-$C_5Me_4SiMe_2$-$NCH_2CH_2OMe)_2$] (1a).** Clear, colorless crystals suitable for X-ray diffraction analysis were obtained by slow evaporation of $C_6D_6$ from a concentrated solution; an ORTEP diagram of the structure of **1a** is shown in Figure 7.[33] Crystallographic data are compiled in Table 1.

The yttrium atom is coordinated in a pseudotetrahedral fashion by a pair of cyclopentadienyl and amido

(27) Epimerizations of 18-electron organometallics usually proceed through a dissociative mechanism with initial loss of a monodentate ligand, such as phosphine, giving a stereochemical nonrigid intermediate, and recoordination of the donor ligand, see: (a) Dewey, M. A.; Stark, G. A.; Gladysz, J. A. *Organometallics* **1996**, *15*, 4798. (b) Dewey, M. A.; Bakke, J. M.; Gladysz, J. A. *Organometallics* **1990**, *9*, 1351. (c) Brunner, H.; Fisch, K.; Jones, P. G.; Salbeck, J. *Angew. Chem., Int. Ed. Engl.* **1989**, *28*, 1521. (d) Martin, G. C.; Boncella, J. M. *Organometallics* **1989**, *8*, 2968. (e) Brunner, H. *Top. Curr. Chem.* **1975**, *56*, 67 and references cited therein.

(28) Giardello, M. A.; Conticello, V. P.; Brard, L.; Sabat, M.; Rheingold, A. L.; Stern, C. L.; Marks, T. J. *J. Am. Chem. Soc.* **1994**, *116*, 10212.

(29) (a) Diamond, G. M.; Jordan, R. F.; Petersen, J. L. *Organometallics* **1996**, *15*, 4045. (b) Christopher, J. N.; Diamond, G. M.; Jordan, R. F.; Petersen, J. L. *Organometallics* **1996**, *15*, 4038.

(30) $Me_2Si(1\text{-}C_5H_3\text{-}3\text{-}tBu)_2Zr(NMe_2)_2$ was synthesized in a *rac*/*meso* ratio of 1/2, see ref 29a. Synthesis of the corresponding dichloro complex via metathesis gave a *rac*/*meso* ratio of 1/1, see ref 25, whereas the synthesis of the scandium and neodymium analogues gave solely the *meso*-isomer, see: (a) Bunel, E.; Burger, B. J.; Bercaw, J. E. *J. Am. Chem. Soc.* **1988**, *110*, 976. (b) Esser, L. Ph.D. Dissertation, Technische Universität Berlin, Germany, 1991.

(31) For photoisomerization of *ansa*-metallocenes see: (a) Wild, F. R. W. P.; Zsolnai, L.; Huttner, G.; Brintzinger, H. H. *J. Organomet. Chem.* **1982**, *232*, 233. (b) Collins, S.; Hong, Y.; Taylor, N. J. *Organometallics* **1990**, *9*, 2695. (c) Collins, S.; Hong, Y.; Ramachandran, R.; Taylor, N. J. *Organometallics* **1991**, *10*, 2349. (d) Rheingold, A. L.; Robinson, N. P.; Whelan, J.; Bosnich, B. *Organometallics* **1992**, *11*, 1869. (e) Kaminsky, W.; Schauwienold, A.-M.; Freidanck, F. *J. Mol. Catal. A: Chemical* **1996**, *112*, 37.

(32) Zsolnai, L.; Pritzkow, H. *ZORTEP Ortep Program for PC*; Universität Heidelberg: Heidelberg, Germany, 1994.

(33) The crystal structure of the lutetium complex **2a** is analogous to the yttrium compound and could be solved by isotypic replacement of the structure of **1a**. The $Cp_{Cent}$−Lu (2.356(5) and 2.364(5) Å) and Lu−N (2.272(4) and 2.275(4) Å) bond distances, as well as $Cp_{Cent}$−Lu−$Cp_{Cent}$ (136.9(2)°), are slightly smaller than in **1a**. Full crystallographic data and an ORTEP diagram of the structure of **2a** are given in the Supporting Information.

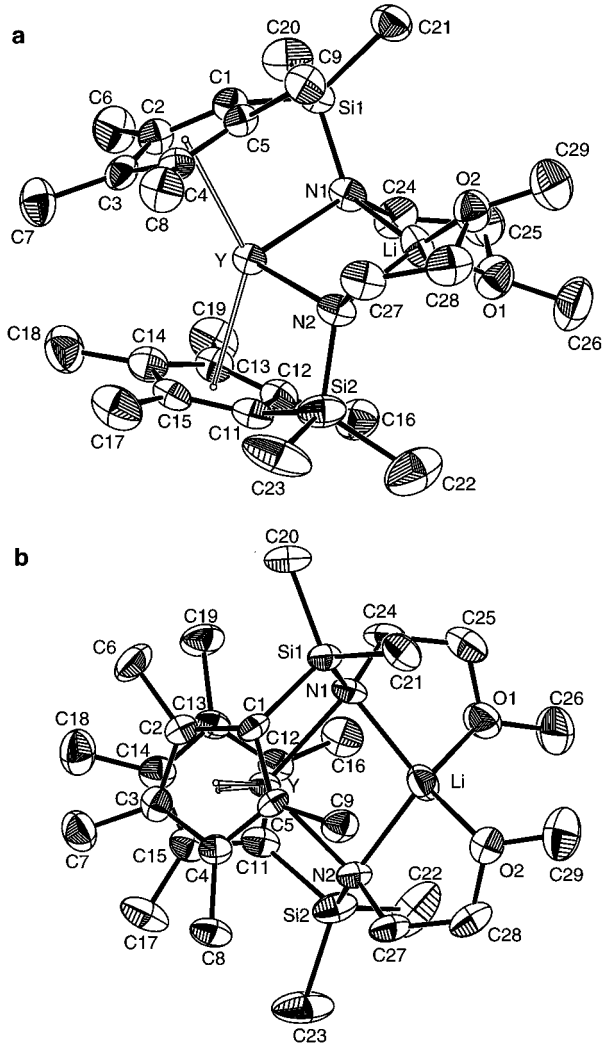


**Figure 7.** (a) ORTEP diagram[32] of the molecular structure of **1a**. (b) Alternative view from the top. Thermal ellipsoids are drawn at the 50% probability level. Hydrogen atoms are omitted for the sake of clarity. Selected bond lengths (Å) and bond angles (deg): Y−N1 2.319(4), Y−N2 2.329(4), Y···Li 2.900(11), O1−Li 1.915(11), O2−Li 1.956(11), N1−Li 2.142(12), N2−Li 2.121(11), $Cp_{Cent}$−Y−$Cp_{Cent}$ 137.7(2), $Cp_{Cent}$1−Y−N1 95.7(2), $Cp_{Cent}$2−Y−N2 95.6(2), $Cp_{Cent}$1−Y−N2 112.9(2), $Cp_{Cent}$2−Y−N1 113.9(2), N1−Y−N2 93.1(2).

ligands. The angles at the yttrium center vary from 93.1(2)° (N1−Y−N2) to 137.7(2)° ($Cp_{Cent}$-Y-$Cp_{Cent}$). The Y−C(Cp) bond lengths (2.581(5)−2.765(5) Å) are significantly longer than those reported for Y($\eta^5$:$\eta^1$-$C_5Me_4$-$SiMe_2NCMe_3$){$N(SiMe_3)_2$} (2.535(9)−2.665(10) Å)[11] but are comparable to those in other cyclopentadienyl yttrium complexes.[34] They display a pattern similar to that found in ring-bridged organolanthanide complexes[2d,28,35] with longer Y−C(Cp) bond distances to carbon atoms distal to the silicon bridge (C3, C4, C13, C14) as compared to that for the proximal carbon atoms (C1, C2, C15, C11). Likewise, the metal−ring centroid ($Cp_{Cent}$) distances in **1a** of 2.392(6) and 2.399(6) Å are comparable to those in unbridged cyclopentadienyl yttrium complexes.[36] The angle $Cp_{Cent}$−Y−$Cp_{Cent}$ (137.7(2)°) lies in the range of other yttrocene complexes.[37] The $Cp_{Cent}$−Y−N angle ($Cp_{Cent}$ and N of the same ligand $Cp_{Cent}$1−Y−N1 = 95.7(2)°; $Cp_{Cent}$2−Y−N2 = 95.6(2)°) resembles the corresponding angle in Y($\eta^5$:$\eta^1$-$C_5Me_4SiMe_2NCMe_3$){$N(SiMe_3)_2$} (97.7°),[11] whereas the angles between different ligands ($Cp_{Cent}$1−Y−N2 = 112.9(2)°; $Cp_{Cent}$2−Y−N1 = 113.9(2)°) correspond to that in $Cp^*_2YN(SiMe_3)_2$ (112.0(2)−114.6(2)°).[34a] The Y−N bond lengths are substantially longer than those reported for many yttrium amide complexes (Table 2). The short Y−N bond lengths in such yttrium amide complexes have been explained by a dative $\pi$-bonding between the nitrogen lone pair and the Lewis acidic yttrium atom. In **1a**, however, only one lone pair of electrons can be accommodated in the empty $a_1$ orbital of the $Cp_2MX_2$ unit,[40] thus leaving the second electron pair formally localized on the amido nitrogen atoms. Consequently, the geometry of the nitrogen atom is somewhat between trigonal planar ($sp^2$) and pyramidal ($sp^3$) with a longer metal−nitrogen bond length. In agreement with this bonding situation, the amido-nitrogen atoms reside in a distorted tetrahedral environment. The bond angles vary from 102.2(2)° (Si1−N1−Y) to 133.0(4)° (C24−N1−Y). They show deviation from planarity in contrast to other structurally characterized amido-functionalized cyclopentadienyl complexes. The sum of the bond angles at the nitrogen of 350.7(3)° and 351.3(3)° are smaller than 360°, which is typical for an $sp^2$-hybridized nitrogen atom.

The side chains of the amido-functionalized cyclopentadienyl ligand coordinate the lithium atom in a distorted tetrahedral fashion. The O−Li−N angles show the largest deviation from ideal tetrahedral geometry. The bond angles in the five-membered chelate rings (O1−Li−N1 = 89.3(5)° and O2-Li-N2 = 89.5(5)°) are significantly smaller, whereas the other two angles (O1−Li−N2 = 134.3(6)° and O2−Li−N1 = 137.5(6)°) are

(34) (a) $Cp^*_2YN(SiMe_3)_2$ Y−C(Cp) = 2.632(7)−2.737(7) Å, see: den Haan, K. H.; de Boer, J. L.; Teuben, J. H.; Spek, A. L.; Kojic-Prodic, B.; Hays, G. R.; Huis, R. *Organometallics* **1986**, *5*, 1726. (b) (*R*)-$Me_2SiC_5Me_4$[(−)-menthylCp]$YN(SiMe_3)_2$ Y−C(Cp) = 2.59(1)−2.81(1) Å, see: ref 28. (c) $Cp^*_2Y(\mu$-Cl)$YClCp^*_2$ Y−C(Cp) = 2.56(2)−2.69(2) Å, see: Evans, W. J.; Peterson, T. T.; Rausch, M. D.; Hunter, W. E.; Zhang, H.; Atwood, J. L. *Organometallics* **1985**, *4*, 554. (d) $[Cp_2YMe]_2$ Y−C(Cp) = 2.621(10)−2.683(9) Å, see: Holton, J.; Lappert, M. F.; Ballard, D. G. H.; Pearce, R.; Atwood, J. L.; Hunter, W. E. *J. Chem. Soc., Dalton Trans.* **1979**, 54. (e) $Cp_3Y(THF)$ Y−C(Cp) = 2.65(1)−2.766(7) Å, see: Rogers, R. D.; Atwood, J. L.; Emad, A.; Sikora, P. J.; Rausch, M. D. *J. Organomet. Chem.* **1981**, *216*, 383.

(35) (a) Stern, D.; Sabat, M.; Marks, T. J. *J. Am. Chem. Soc.* **1990**, *112*, 9558. (b) Schumann, H.; Esser, L.; Loebel, J.; Dietrich, A.; van der Helm, D.; Ji, X. *Organometallics* **1991**, *10*, 2585. (c) Schaefer, W. P.; Köhn, R. D.; Bercaw, J. E. *Acta Crystallogr.* **1992**, *C48*, 251. (d) Marsh, R. E.; Schaefer, W. P.; Coughlin, E. B.; Bercaw, J. E. *Acta Crystallogr.* **1992**, *C48*, 1773. (e) Piers, W. E.; Ferguson, G.; Gallagher, J. F. *Inorg. Chem.* **1994**, *33*, 3784. (f) Coughlin, E. B.; Henling, L. M.; Bercaw, J. E. *Inorg. Chim. Acta* **1996**, *242*, 205.

(36) (a) $Cp^*_2Y[N(Ar)$═$C(Ph)C(Ph)$═$N(Ar)]$ $Cp_{Cent}$−Y = 2.408(4) Å, see: Scholz, A.; Thiele, K.-H.; Scholz, J.; Weimann, R. *J. Organomet. Chem.* **1995**, *501*, 195. b) $Cp^*Y(OAr)_2$ $Cp_{Cent}$−Y = 2.363(3) Å, see: Schaverien, C. J.; Frijns, J. H. G.; Heeres, H. J.; van den Hende, J. R.; Teuben, J. H.; Spek, A. L. *J. Chem. Soc., Chem. Commun.* **1991**, 642. (c) $Cp^*[PhC(NSiMe_3)_2]Y(\mu$-Me$)_2$Li(TMEDA) $Cp_{Cent}$−Y = 2.392(3) Å, see: Duchateau, R.; Meetsma, A.; Teuben, J. H. *Organometallics* **1996**, *15*, 1656. (d) $[Cp^*Y(\mu$-O*t*Bu$)$(O*t*Bu$)]_2$ $Cp_{Cent}$−Y = 2.415 Å, see: Evans, W. J.; Boyle, T. J.; Ziller, J. W. *Organometallics* **1993**, *12*, 3998.

(37) Evans, W. J.; Foster, S. E. *J. Organomet. Chem.* **1992**, *433*, 79.

(38) Westernhausen, M.; Hartmann, M.; Pfitzner, A.; Schwarz, W. *Z. Anorg. Allg. Chem.* **1995**, *621*, 837.

(39) (a) Evans, W. J.; Meadows, J. H.; Hunter, W. E.; Atwood, J. L. *J. Am. Chem. Soc.* **1984**, *106*, 1291. (b) Evans, W. J.; Meadows, J. H.; Hunter, W. E.; Atwood, J. L. *Organometallics* **1983**, *2*, 1252. (c) Lee, L.; Berg, D. J.; Bushnell, G. W. *Inorg. Chem.* **1994**, *33*, 5302.

(40) Lauher, J. W.; Hoffmann, R. *J. Am. Chem. Soc.* **1976**, *98*, 1729. The bis(amido) anion $[Cp_2Ln(NPh_2)_2]^-$ shows the same feature, see: Schumann, H.; Palamidis, E.; Loebel, J. *J. Organomet. Chem.* **1990**, *390*, 45. Guan, J.; Shen, Q.; Jin, S.; Lin, Y. *Polyhedron* **1994**, *13*, 1695. In some $d^0$-$Cp_2MX_2$ complexes where X is a $\pi$-donor such as $PR_2$, localization of a single and double bond was observed, see: Baker, R. T.; Whitney, J. F.; Wreford, S. S. *Organometallics* **1983**, *2*, 1049.

**Table 1. Experimental Data of the Crystal Structure Determination of Li[Y($\eta^5$:$\eta^1$-$C_5Me_4SiMe_2NCH_2CH_2OMe)_2$]·$C_6D_6$ (1a), (*R,S*)-Li[Y($\eta^5$:$\eta^1$-$C_5H_3t$BuSi$Me_2NCH_2CH_2OMe)_2$]·$^1/_2C_6H_6$ ((*R,S*)-3a), and (*R,R*)-Li[Y($\eta^5$:$\eta^1$-$C_5H_3t$BuSi$Me_2NCH_2CH_2NMe_2)_2$] ((*R,R*)-3b)**

| | 1a | (*R,S*)-3a | (*R,R*)-3b |
|---|---|---|---|
| | Crystal Data | | |
| empirical formula | $C_{28}H_{50}LiN_2O_2Si_2Y·C_6D_6$ | $C_{28}H_{50}LiN_2O_2Si_2Y·^1/_2C_6H_6$ | $C_{30}H_{56}LiN_4Si_2Y$ |
| fw | 682.89 | 637.78 | 624.82 |
| cryst color | colorless | colorless | colorless |
| cryst size, mm | 0.2 × 0.3 × 0.5 | 0.5 × 0.4 × 0.4 | 0.2 × 0.4 × 0.4 |
| cryst system | orthorhombic | triclinic | monoclinic |
| space group | $P2_12_12_1$ (No. 19) | $P\bar{1}$ (No. 2) | $C2/c$ (No. 15) |
| *a*, Å | 12.024(5) | 10.273(2) | 11.642(2) |
| *b*, Å | 16.284(4) | 13.477(3) | 16.323(5) |
| *c*, Å | 18.775(5) | 13.740(2) | 18.416(3) |
| α, deg | 90 | 97.61(2) | 90 |
| *β*, deg | 90 | 107.25(1) | 94.07(2) |
| *γ*, deg | 90 | 93.56(2) | 90 |
| *V*, Å$^3$ | 3676(2) | 1790.4(6) | 3491(1) |
| *Z* | 4 | 2 | 8/2 |
| $\rho_{calcd}$, g cm$^{-3}$ | 1.234 | 1.183 | 1.189 |
| $\mu$(Mo Kα), mm$^{-1}$ | 1.681 | 1.722 | 1.762 |
| *F*(000) | 1440 | 678 | 1336 |
| | Data Collection | | |
| wavelength | Mo Kα (0.710 70 Å) | Mo Kα (0.710 70 Å) | Mo Kα (0.710 70 Å) |
| *T*, K | 223(2) | 296(2) | 296(2) |
| *θ* range | 3−28 | 3−28 | 3−30 |
| index ranges | *h*, −13 to 13; *k*, −17 to 21; *l*, −20 to 24 | *h*, 0 to 13; *k*, −17 to 17; *l*, −18 to 17 | *h*, −16 to 16; *k*, −18 to 22; *l*, −25 to 25 |
| | Solution and Refinement | | |
| no. of rflns measd | 6739 | 9074 | 13 894 |
| no. of indep rflns | 6082 ($R_{int}$ = 0.0337) | 8599 ($R_{int}$ = 0.0297) | 4359 ($R_{int}$ = 0.0418) |
| no. of obsd rflns | 4570 ($I > 2\sigma(I)$) | 5377 ($I > 2\ \sigma(I)$) | 2794 ($I > 2\ \sigma(I)$) |
| GOF | 1.17 | 1.04 | 1.12 |
| R | 0.046 | 0.051 | 0.039 |
| $wR_2$ ($I > 2\sigma(I)$) | 0.088 | 0.091 | 0.073 |
| largest *e*-max, *e*-min, e·Å$^{-3}$ | 0.409, −0.736 | 0.468, −0.344 | 0.414, −0.379 |
| abs struct param | −0.040(8) | | |

**Table 2. Comparison of Y−N Bond Distances in Yttrium Amide Complexes**

| compd | Y−N, Å | ref |
|---|---|---|
| **1a** | 2.319(4), 2.329(4) | this work |
| **(*R,S*)-3a** | 2.333(3), 2.318(3) | this work |
| **(*R,R*)-3b** | 2.330(2) | this work |
| Y($\eta^5$:$\eta^1$-$C_5Me_4SiMe_2Nt$Bu){$N(SiMe_3)_2$} | Y−N$SiMe_2$ = 2.184(7), Y−N$(SiMe_3)_2$ = 2.255(8) | 11 |
| $Cp^*_2YN(SiMe_3)_2$ | 2.274(5), 2.253(5) | 34a |
| (*R*)-$Me_2SiC_5Me_4$[(−)-menthylCp]Y$N(SiMe_3)_2$ | 2.281(8), 2.211(8) | 28 |
| [Li(THF)$_4$][Y{$N(SiMe_3)_2$}$_3$Cl] | 2.25 average | 38 |
| [Y{$N(SiMe_3)_2$}$_3$(NCPh)$_2$] | 2.248(4)−2.265(4) | 38 |
| $Cp^*_2$Y[N(Ar)=C(Ph)C(Ph)=N(Ar)] | 2.362(6) | 36a |
| [$Cp_2$Y($\mu$-NCH$t$Bu)]$_2$ | 2.314(9), 2.382(9) | 39a |
| [$Cp_2$Y($\eta^2$-CH=N$t$Bu)]$_2$ | 2.325(4) | 39b |
| Y[DAC][$N(SiMe_3)_2$][a] | Y−N$(SiMe_3)_2$ = 2.338(11), Y−N(DAC) = 2.283(12), 2.29(2) | 39c |

[a] DAC = 4,13-Diaza-18-crown-6.

significantly larger than the ideal tetrahedral angle.[41] The Li−N and Li−O bond lengths show no large deviation from those found in other lithium cryptand complexes.[41,42]

**Molecular Structure of (*R,S*)-Li[Y($\eta^5$:$\eta^1$-$C_5H_3t$Bu-Si$Me_2NCH_2CH_2OMe)_2$] ((*R,S*)-3a) and (*R,R*)-Li[Y($\eta^5$:$\eta^1$-$C_5H_3t$BuSi$Me_2NCH_2CH_2NMe_2)_2$] ((*R,R*)-3b).** Clear, colorless crystals suitable for X-ray diffraction analysis of **(*R,S*)-3a** and **(*R,R*)-3b** were obtained by slow evaporation of benzene from a concentrated solution; ORTEP diagrams of the structure of **(*R,S*)-3a** and **(*R,R*)-3b** are shown in Figures 8 and 9, respectively. Crystallographic data are compiled in Table 1. These complexes show the same basic structural features as **1a**. The molecular structure of **(*R,R*)-3b** shows a positional disorder with two split positions for C13 and C15 (each with 50% occupancy). For the sake of clarity only one position is shown in Figure 9.

The structure of complex **(*R,R*)-3b** is $C_2$-symmetric with the *tert*-butyl substituents on the two cyclopentadienyl ligands being oriented trans to each other, whereas complex **(*R,S*)-3a** adopts a $C_1$-symmetric structure with one *tert*-butylcyclopentadienyl ligand having the sterically more demanding (*S*)-configuration. The steric hindrance in **(*R,S*)-3a** is evident from a significantly larger $Cp_{Cent}$−Y-$Cp_{Cent}$ angle (140.7(1)°) in **(*R,S*)-3a** than that in **(*R,R*)-3b** (128.9(1)°), **1a**, or in other yttrocene complexes.[37,43] The Y−C(Cp) bond lengths of

(41) A similar situation is found in [(*R,R*)-LiN(CHPh$CH_2$OMe)]$_2$, whose crown ether like structure can be compared with that in **1a**, see: Barr, D.; Berrisford, D. J.; Jones, R. V. H.; Slawin, A. M. Z.; Snaith, R.; Stoddart, J. F.; Williams, D. J. *Angew. Chem., Int. Ed. Engl.* **1989**, *28*, 1044.

(42) (a) Moras, D.; Weiss, R. *Acta Crystallogr.* **1973**, *B29*, 400. (b) Abou-Hamdan, A.; Hounslow, A. M.; Lincoln, S. F.; Hambley, T. W. *J. Chem. Soc., Dalton Trans.* **1987**, 489. (c) Amaudet, L.; Charpin, P.; Folcher, G.; Lance, M.; Nierlich, M.; Vigner, D. *Organometallics* **1986**, *5*, 270. (d) Groth, P. *Acta Chem. Scand.* **1985**, *A39*, 73.

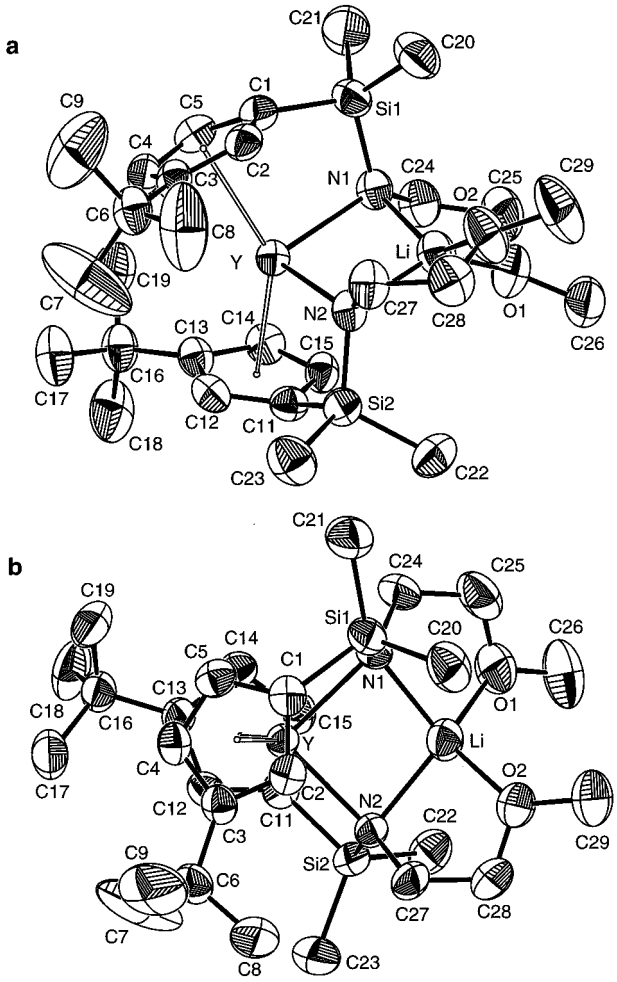


**Figure 8.** (a) ORTEP diagram[32] of the molecular structure of **(*R*,*S*)-3a**. (b) Alternative view from the top. Thermal ellipsoids are drawn at the 50% probability level. Hydrogen atoms are omitted for the sake of clarity. Selected bond lengths (Å) and bond angles (deg): Y−N1 2.333(3), Y−N2 2.318(3), Y···Li 2.976(6), O1−Li 1.937(7), O2−Li 1.930(7), N1−Li 2.123(7), N2−Li 2.121(7), $Cp_{Cent}$−Y−$Cp_{Cent}$ 140.7(1), $Cp_{Cent}1$−Y−N1 96.1(1), $Cp_{Cent}2$−Y−N2 95.4(1), $Cp_{Cent}1$−Y−N2 113.7(1), $Cp_{Cent}2$−Y−N1 110.3(1), N1−Y−N2 90.0(1).

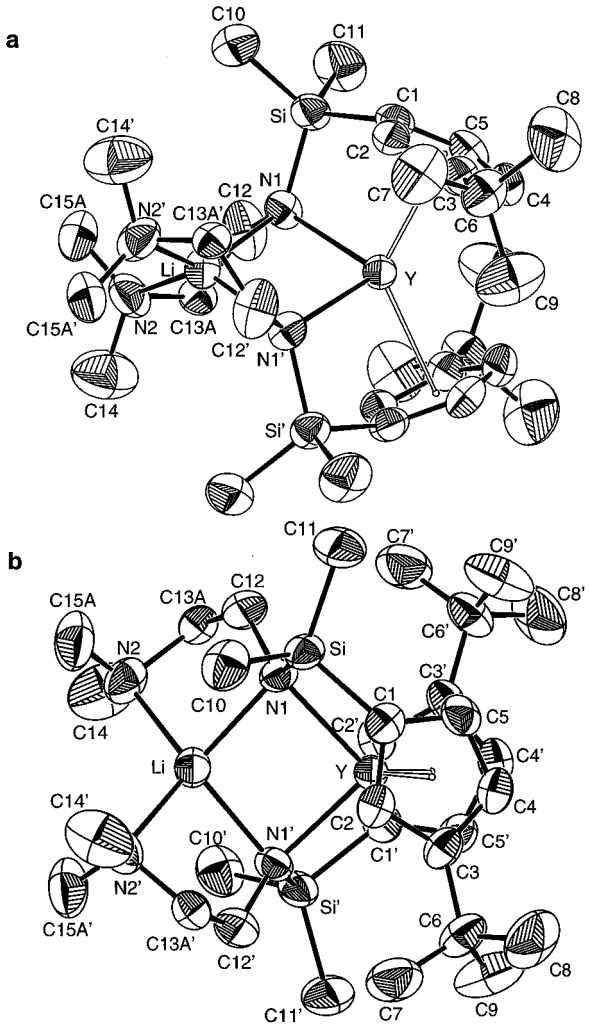


**Figure 9.** (a) ORTEP diagram[32] of the molecular structure of **(*R*,*R*)-3b**. (b) Alternative view from the top. Thermal ellipsoids are drawn at the 50% probability level. The atoms marked with primes are constructed through rotation by the 2-fold axis. Hydrogen atoms and one position of the disordered atoms C13 and C15 are omitted for the sake of clarity. Selected bond lengths (Å) and bond angles (deg): Y−N1 2.330(2), Y···Li 3.059(6), N1−Li 2.200(5), N2−Li 2.111(4), $Cp_{Cent}$−Y−$Cp_{Cent}$ 128.9(1), $Cp_{Cent}$−Y−N1 96.8(1), $Cp_{Cent}$−Y−N1′ 118.9(1), N1−Y−N1′ 91.53(11).

**(*R*,*S*)-3a** (2.578(3)−2.806(3) Å) and **(*R*,*R*)-3b** (2.575(3)−2.830(3) Å) display a similar pattern to that in **1a**. The $Cp_{Cent}$−Y−N angles are comparable to that in **1a**, however, the angle between different ligands in **(*R*,*R*)-3b** ($Cp_{Cent}1$−Y−N1′ = 118.9(1)°) is significantly larger than that in **1a** and **(*R*,*S*)-3a**, as expected from the smaller $Cp_{Cent}$−Y−$Cp_{Cent}$ angle. The $Cp_{Cent}$−Y distances (**(*R*,*S*)-3a** 2.403(3) and 2.390(3) Å; **(*R*,*R*)-3b** 2.405(3) Å) and Y−N bond lengths (see Table 2) are comparable to those found in **1a**. The bond length of lithium to the amide-nitrogen atom in **(*R*,*R*)-3b** (Li−N1 = 2.200(5) Å) is slightly longer than the bond to the amine-nitrogen atom (Li−N2 = 2.111(4) Å) and also to the corresponding bond in **1a**, indicating a stronger lithium amine bond at the expense of the lithium amide bond.

**Polymerization.** Complexes **1**−**3** were found to catalyze the ring-opening polymerization of ϵ-caprolactone in toluene or dichloromethane at room temperature, with different activities. When the polymerization is performed in toluene, solutions become highly viscous and magnetic stirring is impeded within a few minutes in the case of **1** and within 30 min in the case of **3b**. When dichloromethane is used as the solvent, the solutions remain fluid.[44] After the solution is quenched with methanol, the poly(ϵ-caprolactone)s were isolated as colorless solids and characterized by gel permeation

(43) (a) [$(Me_3SiC_5H_4)_2Y(\mu\text{-Cl})]_2$ $Cp_{Cent}$−Y−$Cp_{Cent}$ = 130.1°, see: Evans, W. J.; Sollberger, M. S.; Shreeve, J. L.; Olofson, J. M.; Hain, J. H., Jr.; Ziller, J. W. *Inorg. Chem.* **1992**, *31*, 2492. (b) [$(t\text{BuC}_5H_4)_2Y(\mu\text{-SePh})]_2$ $Cp_{Cent}$−Y−$Cp_{Cent}$ = 127.7(3)°, see: Beletskaya, I. P.; Voskoboynikov, A. Z.; Shestakova, A. K.; Yanovsky, A. I.; Fukin, G. K.; Zacharov, L. N.; Struchkov, Y. T.; Schumann, H. *J. Organomet. Chem.* **1994**, *468*, 121. (c) [$(t\text{BuC}_5H_4)_2Y(C_4H_7S_2\text{-}1,3)$]·LiCl·2THF $Cp_{Cent}$−Y−$Cp_{Cent}$ = 126.5(8)°, see: Vinogradov, S. A.; Mistrukov, A. E.; Beletskaya, I. P. *J. Chem. Soc., Dalton Trans.* **1995**, 2679.

(44) This increase in viscosity might be due to formation of a coordinative polymer network. Upon addition of 2 mL of methanol, the gel becomes liquid again. See: Schlaad, H.; Müller, A. H. E. *Polymer J.* **1996**, *28*, 954. Therefore, a decrease of the rate of polymerization for some active sites should result in a broadening of the molecular weight distribution. This could also explain the lower polydispersities obtained in dichloromethane.

**Table 3. Polymerization of ϵ-Caprolactone by the Heterobimetallic Complexes[a]**

| entry | cat | time (h) | solvent | [monomer]/[cat] | yield, % | $M_n(\times 10^3)$, g/mol | $M_w(\times 10^3)$, g/mol | $M_w/M_n$ |
|---|---|---|---|---|---|---|---|---|
| 1 | **1a**[b] | 1.5 | toluene | 42 | 85 | 58 | 112 | 1.9 |
| 2 | **1a** | 1.5 | toluene | 90 | 78 | 34 | 53 | 1.6 |
| 3 | **1a** | 1.5 | toluene | 147 | 82 | 44 | 67 | 1.5 |
| 4 | **1a**[c] | 1.5 | toluene | 188 | 92 | 177 | 333 | 1.9 |
| 5 | **1a** | 1.5 | toluene | 197 | 92 | 39 | 72 | 1.8 |
| 6 | **1a** | 1.5 | $CH_2Cl_2$ | 183 | 75 | 14 | 19 | 1.4 |
| 7 | **1b** | 1.5 | toluene | 199 | 94 | 94 | 159 | 1.7 |
| 8 | **2a** | 5 | toluene | 221 | 42 | 14 | 16 | 1.1 |
| 9 | **2a** | 42 | $CH_2Cl_2$ | 180 | 89 | 11 | 14 | 1.3 |
| 10 | **3a**[d] | 1.5 | toluene | 220 | 93 | 76 | 135 | 1.8 |
| 11 | **3a**[e] | 1.5 | toluene | 245 | 91 | 51 | 83 | 1.6 |
| 12 | **3b**[f] | 1.5 | toluene | 246 | 91 | 31 | 50 | 1.6 |
| 13 | **3b**[g] | 1.5 | toluene | 230 | 89 | 80 | 141 | 1.8 |
| 14 | $Y\{N(SiMe_3)_2\}_3$ | 1.5 | toluene | 224 | 65 | 524 | 1509 | 2.9 |

[a] [cat] = $5 \times 10^{-3}$ mol $L^{-1}$. [b] [cat] = $42 \times 10^{-3}$ mol $L^{-1}$. [c] [cat] = $10 \times 10^{-3}$ mol $L^{-1}$. [d] (*R,R*):(*R,S*) = 1:6. [e] (*R,R*):(*R,S*) = 1.7:1. [f] (*R,R*):(*R,S*) = 1:5. [g] (*R,R*):(*R,S*) = 3.5:1.

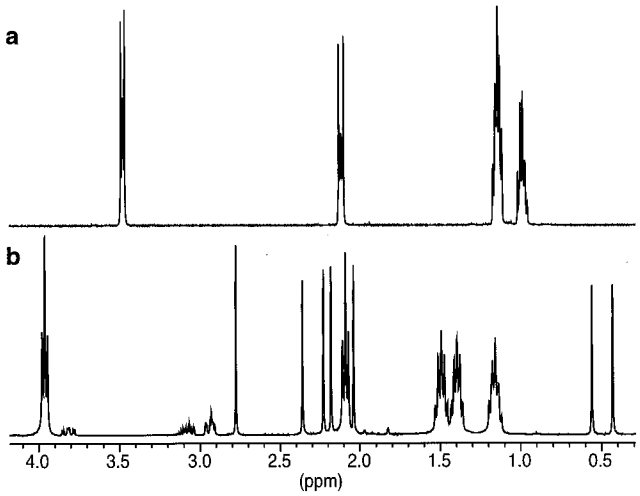


**Figure 10.** (a) $^1$H NMR spectrum of ϵ-caprolactone in $C_6D_6$ at 25 °C. (b) $^1$H NMR spectrum of **2a** with 6 equiv of ϵ-caprolactone in $C_6D_6$ at 25 °C after 30 min.

chromatography. The results are summarized in Table 3.

The polymers formed by **1**−**3** are generally of high molecular weight ($M_n$ > 30 000) and show moderate polydispersities ($M_w/M_n$ < 2.0). The lutetium complex **2a** is the least effective catalyst, possibly due to the smaller ionic radius of lutetium compared to that of yttrium, but the polymer formed shows the lowest value of polydispersity. The homoleptic tris(amide) $Y\{N(SiMe_3)_2\}_3$[11] was also found to polymerize ϵ-caprolactone, but the molecular weight distribution of the resulting poly(ϵ-caprolactone) is much broader than those found for polymers formed by complexes **1**−**3**. This may be caused by the monodentate amido ligands and the absence of an inert spectator ligand. A similar observation has been made using the divalent complex $Sm\{N(SiMe_3)_2\}_2(THF)_2$.[5c]

In order to learn more about the polymerization mechanism, the complexes **1a**, **2a**, and **(*R,S*)-3a** were treated with ϵ-caprolactone in the range from 2 to 30 equiv in a NMR tube. The $^1$H NMR spectrum recorded after 30 min shows the unchanged spectrum of the bis(ligand) complex and signals arising from poly(ϵ-caprolactone) (Figure 10). Intriguingly, no end-group signal could be detected. When ϵ-caprolactone is used in higher concentrations (>5 equiv), the solution becomes highly viscous and the initial $^1$H NMR spectrum taken 10 min after mixing shows signals arising from monomeric ϵ-caprolactone, which disappear within 1 h. No other species were detected by $^1$H NMR spectroscopy. Gel permeation chromatography analysis of the tube contents with 30 equiv of ϵ-caprolactone showed $M_n$ = 6700, $M_w$ = 11 300, and $M_w/M_n$ = 1.7.

As the initial step of the polymerization, one can envisage a nucleophilic attack by one of the nucleophilic amido-nitrogen atoms at the lactone carbonyl-carbon atom, followed by acyl bond cleavage and formation of an alkoxide. The fact that the nucleophilic amido-nitrogen atom is the attacking species, and not the cyclopentadienyl ligand, can be concluded from the polymerization of ϵ-caprolactone with **(*R,S*)-3a**, which occurs with retention of configuration at the planar chiral cyclopentadienyl ligand in **(*R,S*)-3a**. As indicated in Scheme 4, the alkoxo group is assumed to be bonded to both yttrium and lithium, a bonding situation analogous to that for the two amido groups in the starting complex. It opens up a coordination site at the yttrium when monomeric ϵ-caprolactone approaches through the carbonyl-oxygen atom. Models for this interaction can be found in the crystallographically characterized ϵ-caprolactone complex *mer*-$YCl_3$(ϵ-caprolactone)$_3$[45] and the $^1$H NMR spectroscopically identified initiator complex ($\eta^5$-$C_5Me_5)_2Y$(OMe)(ϵ-caprolactone).[5b] The chain termination would be the attack of the alkoxide at the amide bond with formation of cyclic polymers and back-formation of the catalyst. There is at least one precedence for the reaction at the silylamido link, *viz.* the carboxylation of Zr($\eta^5$:$\eta^1$-$C_5Me_4SiMe_2NCMe_3$)$Me_2$ to give dimeric [Zr($\eta^5$:$\eta^1$-$C_5Me_4SiMe_2O$)($\eta^2$-$O_2CMe)_2]_2$ and of Ti($\eta^5$:$\eta^1$-$C_5H_4SiMe_2NR)Cl_2$ to give [Ti($\eta^5$:$\eta^1$-$C_5H_4SiMe_2O)Cl_2]_2$.[46] This reaction step seems to be irreversible, since no reaction occurs when **2a** is treated with 8 equiv of the cyclic dimer of ϵ-caprolactone[47] in $C_6D_6$ after 24 h at room temperature, as judged by NMR spectroscopy. The mechanism for the polymerization of ϵ-caprolactone proposed here differs from the common quasi-anionic ring-opening mechanism.[1,4c,6a,7e] Since we failed to detect any linear correlation of the molecular weight with the monomer:initiator ratio, a catalytic polymerization similar to a radical polymerization seems to be

(45) (a) Evans, W. J.; Shreeve, J. L.; Doedens, R. J. *Inorg. Chem.* **1993**, *32*, 245. (b) Evans, W. J.; Shreeve, J. L.; Ziller, J. W.; Doedens, R. J. *Inorg. Chem.* **1995**, *34*, 578.

(46) (a) Kloppenburg, L.; Petersen, J. L. *Organometallics* **1996**, *15*, 7. (b) Ciruelos, S.; Cuenca, T.; Gómez, R.; Gómez-Sal, P.; Manzanero, A.; Royo, P. *Organometallics* **1996**, *15*, 5577.

(47) Ito, K.; Hashizuka, Y.; Yamashita, Y. *Macromolecules* **1977**, *10*, 821.

**Scheme 4**

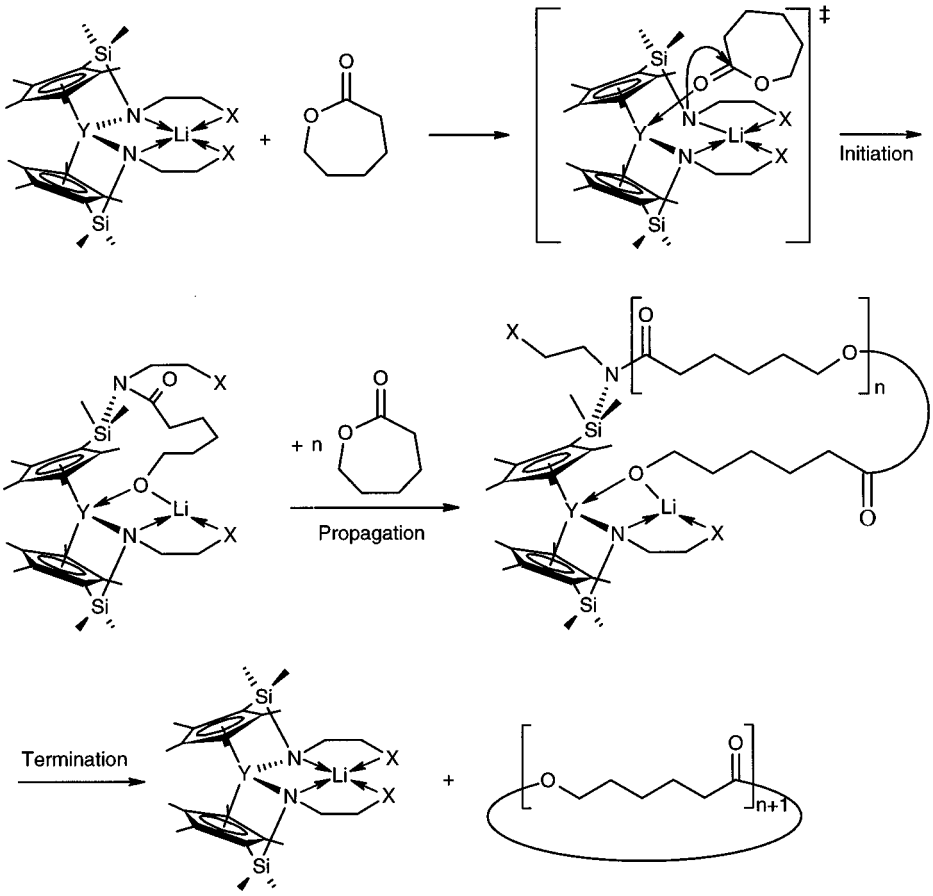


operative. Very fast (on the NMR time scale) initiation, propagation, and termination corroborate this proposal.

## Conclusion

Using tridentate-bridged amido−cyclopentadienyl ligands [$C_5R_4SiMe_2NCH_2CH_2X$], rare earth metal complexes with unique helical heterobimetallic structures of $C_2$-symmetry have been synthesized and structurally characterized. The formal 20-electron configuration at the metal center is "stabilized" by the intramolecular crown ether like coordination of the lithium ion, most clearly evidenced by the significant pyramidalization of the two amido-nitrogen atoms.

In the case of the planar chiral ligand system, where the $C_5R_4$ group is 3-*tert*-butylcyclopentadienyl, two of the three possible diastereomeric pairs are formed. Epimerization of the sterically more constrained $C_1$-symmetric (*R*,*S*)-isomer to give the $C_2$-symmetric (*R*,*R*)-isomer can be observed in THF, reflecting the electronic situation at the $f^{14}$,$d^0$-metal center. The fast ring-opening polymerization of $\epsilon$-caprolactone can be rationalized in terms of the nucleophilic amido bridge, under the possible influence of the heterobimetallic structure. A conceptual resemblance to Shibasaki's lanthanoid tris(BINOL) complexes should be also noted, where the alkali metals assist the activation of substrates.[48]

## Experimental Section

**General Considerations.** All operations were performed under an inert atmosphere of argon using standard Schlenk-line or glovebox techniques. After drying over KOH, THF was distilled from sodium benzophenone ketyl. Hexane and toluene were purified by distillation from sodium/triglyme benzophenone ketyl. $\epsilon$-Caprolactone was dried over $CaH_2$ for 10 days, distilled in vacuo, and stored over molecular sieves. Anhydrous $YCl_3$ and $LuCl_3$ (ALFA) were used as received. $Li_2(C_5Me_4SiMe_2NCH_2CH_2OMe)$, $Li_2(C_5Me_4SiMe_2NCH_2CH_2NMe_2)$, and $Li_2(C_5H_3tBuSiMe_2NCH_2CH_2NMe_2)$[13] were synthesized as described in the literature. All other chemicals were commercially available and used as received unless otherwise stated. $^1H$ and $^{13}C$ NMR spectra were recorded on Bruker AM 400 and DRX 400 spectrometers. Mass spectra were obtained on a Finnigan 8230 spectrometer. The molecular weights of the isolated polymers were determined by gel permeation chromatography at room temperature using THF as the eluent and a universal calibration relative to polystyrene standards. Elemental analyses were performed by the Microanalytical Laboratory of this department.

**$(C_5H_4tBu)SiMe_2(NHCH_2CH_2OMe)$.** To a solution of *tert*-butylcyclopentadiene (5.37 g, 44.0 mmol) in THF (40 mL) was slowly added at −78 °C a solution of *n*-butyllithium (22 mL, 46 mmol, 2.1 M in hexane). The reaction mixture was allowed to warm to room temperature and was stirred for an additional 4 h. The solution was cooled again to −78 °C and chlorodimethylsilane (8 mL) was added. After the reaction mixture was stirred for 1 h, it was allowed to warm to room temperature and stirred overnight. The solvent and excess dichlorodimethylsilane were removed under vacuum (50 mbar, 25 °C). The crude *tert*-butyl(chlorodimethylsilyl)cyclopentadiene was dissolved in hexane (25 mL), filtered from lithium chloride, and added to a suspension of $LiNHCH_2CH_2OMe$ (3.73 g, 46.0 mmol) in hexane (35 mL) at −78 °C. The resulting suspension was allowed to warm to room temperature and stirred overnight. Removal of the solvent and distillation under vacuum (bp 55 °C, 0.03 mbar) gave a colorless oil, yield 9.46 g (85%). $^1H$ NMR ($CDCl_3$, 25 °C): $\delta$ −0.08 (s, 6 H, $SiCH_3$), 1.17 (s, 9 H,

(48) Sasai, H.; Arai, T.; Satow, Y.; Houk, K. N.; Shibasaki, M. *J. Am. Chem. Soc.* **1995**, *117*, 6194.

$C(CH_3)_3$), 2.88 (m, 2 H, $NCH_2$), 3.32 (m, 2 H, $CH_2O$), 3.34 (s, 3 H, $OCH_3$), 6.05, 6.45, 6.61 (m, 1 H, ring H). $^{13}C$ NMR ($CDCl_3$, 25 °C): $\delta$ −3.1 ($SiCH_3$), 30.4 ($CCH_3$), 32.2 ($CCH_3$), 41.7 ($NCH_2$), 52.7 (ring C attached to $SiMe_2$), 58.6 ($OCH_3$), 75.6 ($CH_2O$), 123.2, 124.5, 127.4, 130.3, 133.3, 142.6, 142.8, 155.8 (ring C). EI MS: *m*/*z* 253 (57, $M^+$), 197 (18, $M^+ - C_4H_9$), 179 (19, $M^+ - NHCH_2CH_2OMe$), 132 (69, $M^+ - C_9H_{13}$), 121 (32, $C_9H_{13}^+$), 106 (100, $C_8H_{10}^+$), 91 (77, $C_7H_7^+$), 73 (63, $NCH_2CH_2OMe^+$), 59 (25, $CH_2CH_2OMe^+$), 57 (67, $C_4H_9^+$). Anal. Calcd for $C_{14}H_{27}NOSi$: C, 66.34; H, 10.74; N, 5.53. Found: C, 59.51; H, 9.86; N, 5.10.

**$Li_2(C_5H_3tBuSiMe_2NCH_2CH_2OMe)$.** To a solution of $(C_5H_4tBu)SiMe_2(NHCH_2CH_2OMe)$ (3.65 g, 14.4 mmol) in hexane (30 mL) was added at −78 °C a solution of *n*-butyllithium (14 mL, 29 mmol, 2.1 M in hexane) dropwise. The solution was allowed to warm to room temperature and stirred for 4 h. Removal of the solvent in vacuo gave $Li_2(C_5H_3tBuSiMe_2NCH_2CH_2OMe)$ in quantitative yield as a pale yellow powder.

**Li[Y($\eta^5$:$\eta^1$-$C_5Me_4SiMe_2NCH_2CH_2OMe)_2$] (1a).** $YCl_3$ (391 mg, 2.00 mmol) and $Li_2(C_5Me_4SiMe_2NCH_2CH_2OMe)$ (1.06 g, 4.00 mmol) were combined in a flask, and precooled THF (30 mL) was added at −78 °C with stirring. The resulting mixture was allowed to warm to room temperature and stirred overnight. The solvent was removed in vacuo, and the crude product was extracted with 2 × 20 mL of toluene. LiCl was filtered off, and the clear solution was concentrated to 3 mL. After crystallization at −25 °C for 24 h, the mother liquor was decanted off and the crystals were dried in vacuo to yield 985 mg (82%) of **1a** as colorless microcrystals. $^1H$ NMR ($C_6D_6$, 25 °C): $\delta$ 0.46, 0.59 (s, 6 H, $SiCH_3$), 2.05, 2.15, 2.21, 2.38 (s, 6 H, ring $CH_3$), 2.78 (s, 6 H, $OCH_3$), 2.93 (m, 4 H, $NCH_2CH_2O$), 3.06 (m, 2 H, $CH_2O$), 3.78 (m, 2 H, $NCH_2$). $^{13}C$ NMR ($C_6D_6$, 25 °C): $\delta$ 2.2, 8.4 ($SiCH_3$), 10.7, 12.0, 13.2, 16.0 (ring $CH_3$), 48.1 ($NCH_2$), 58.7 ($OCH_3$), 80.3 ($CH_2O$), 106.4 (ring C attached to $SiMe_2$), 120.3, 121.1, 121.3, 125.2 (ring C). Anal. Calcd for $C_{28}H_{50}LiN_2O_2Si_2Y$: C, 56.17; H, 8.42; N, 4.68. Found: C, 55.46; H, 7.40; N, 4.80.

**Li[Y($\eta^5$:$\eta^1$-$C_5Me_4SiMe_2NCH_2CH_2NMe_2)_2$] (1b).** $YCl_3$ (391 mg, 2.00 mmol) and $Li_2(C_5Me_4SiMe_2NCH_2CH_2NMe_2)$ (1.11 g, 4.00 mmol) were combined in a flask, and precooled THF (30 mL) was added at −78 °C with stirring. The resulting mixture was allowed to warm to room temperature and stirred overnight. The solvent was removed in vacuo, and the crude product was extracted with 2 × 20 mL of toluene. LiCl was filtered off, and the clear solution was concentrated to 5 mL. After crystallization at −25 °C for 24 h, the mother liquor was decanted off and the product dried in vacuo to yield 930 mg (74%) of **1b** as colorless microcrystals. $^1H$ NMR ($C_6D_6$, 25 °C): $\delta$ 0.49, 0.59 (s, 6 H, $SiCH_3$), 1.84 (s, 12 H, $N(CH_3)_2$), 1.88 (dt, $^2J_{H-H}$ = 12.3 Hz, $^3J_{H-H}$ = 2.2 Hz, 2 H, $CH_2NMe_2$), 2.06 (s, 6 H, ring $CH_3$), 2.15 (m, 2 H, $CH_2NMe_2$), 2.17, 2.23, 2.35 (s, 6 H, ring $CH_3$), 3.00 (dt, $^2J_{H-H}$ = 14.4 Hz, $^3J_{H-H}$ = 2.6 Hz, 2 H, $SiNCH_2$), 3.43 (m, 1 H, $SiNCH_2$). $^{13}C$ NMR ($C_6D_6$, 25 °C): $\delta$ 1.7, 10.1 ($SiCH_3$), 10.8, 12.2, 13.4, 16.9 (ring $CH_3$), 46.4 ($SiNCH_2$), 47.1 ($N(CH_3)_2$), 68.0 ($CH_2NMe_2$), 105.3 (ring C attached to $SiMe_2$), 120.4, 121.5, 121.8, 124.1 (ring C). Anal. Calcd for $C_{30}H_{56}LiN_4Si_2Y$: C, 57.67; H, 9.03; N, 8.97. Found: C, 55.42; H, 8.79; N, 8.25.

**Li[Lu($\eta^5$:$\eta^1$-$C_5Me_4SiMe_2NCH_2CH_2OMe)_2$] (2a).** $LuCl_3$ (282 mg, 1.00 mmol) and $Li_2(C_5Me_4SiMe_2NCH_2CH_2OMe)$ (531 mg, 2.00 mmol) were combined in a flask, and precooled THF (15 mL) was added at −78 °C with stirring. The resulting mixture was allowed to warm to room temperature and stirred overnight. The solvent was removed in vacuo, and the crude product was extracted with 2 × 10 mL of toluene. LiCl was filtered off, and the clear solution was concentrated to 2 mL. After crystallization at −25 °C for 48 h, the mother liquor was decanted off and the crystals were dried in vacuo to yield 560 mg (82%) of **2a** as off-white microcrystals. $^1H$ NMR ($C_6D_6$, 25 °C): $\delta$ 0.45, 0.59 (s, 6 H, $SiCH_3$), 2.06, 2.20, 2.26, 2.39 (s, 6 H, ring $CH_3$), 2.76 (s, 6 H, $OCH_3$), 2.94 (m, 4 H, $NCH_2CH_2O$), 3.07 (m, 2 H, $CH_2O$), 3.84 (ddd, $^2J_{H-H}$ = 14.1 Hz, $^3J_{H-H}$ = 12.5 Hz, $^3J_{H-H}$ = 3.7 Hz, 2 H, $NCH_2$). $^{13}C$ NMR ($C_6D_6$, 25 °C): $\delta$ 2.0, 8.3 ($SiCH_3$), 10.8, 12.2, 13.5, 16.3 (ring $CH_3$), 48.5 ($NCH_2$), 58.7 ($OCH_3$), 80.2 ($CH_2O$), 105.5 (ring C attached to $SiMe_2$), 119.0, 120.7, 121.4, 124.3 (ring C). Anal. Calcd for $C_{28}H_{50}LiLuN_2O_2Si_2$: C, 49.11; H, 7.36; N, 4.09. Found: C, 47.98; H, 7.16; N, 4.31.

**Li[Y($\eta^5$:$\eta^1$-$C_5H_3tBuSiMe_2NCH_2CH_2OMe)_2$] (3a).** $YCl_3$ (391 mg, 2.00 mmol) and $Li_2(C_5H_3tBuSiMe_2NCH_2CH_2OMe)$ (1.06 g, 4.00 mmol) were combined in a flask, and precooled THF (30 mL) was added at −78 °C with stirring. The resulting mixture was allowed to warm to room temperature and stirred for 17 h. The solvent was removed in vacuo, and the crude product was extracted with 2 × 20 mL of toluene. LiCl was filtered off, and the clear solution was concentrated to 5 mL. After crystallization at −25 °C for 24 h, the mother liquor was decanted off and the crystals were dried in vacuo to yield 847 mg (71%) of **3a** as white microcrystals. Data for **(*R*,*R*)-3a**: $^1H$ NMR ($C_6D_6$, 25 °C) $\delta$ 0.35, 0.50 (s, 6 H, $SiCH_3$), 1.42 (s, 18 H, $C(CH_3)_3$), 2.79 (s, 6 H, $OCH_3$), 2.90−3.15 (m, 6 H, $NCH_2CH_2O$), 3.49 (m, 2 H, $NCH_2$), 6.16, 6.21, 6.56 ("t", 2 H, ring H); $^1H$ NMR (THF-$d_8$, 21 °C) $\delta$ 0.22 (s, 12 H, $SiCH_3$), 1.25 (s, 18 H, $C(CH_3)_3$), 3.49 (s, 6 H, $OCH_3$), 5.74, 5.93, 6.34 ("t", 2 H, ring H). $^{13}C$ NMR ($C_6D_6$, 25 °C) $\delta$ −3.0, 2.9 ($SiCH_3$), 32.3 ($C(CH_3)_3$), 33.1 ($C(CH_3)_3$), 52.4 ($NCH_2$), 58.7 ($OCH_3$), 79.0 ($OCH_2$), 112.2, 112.3, 113.0, 114.3 (ring C), 142.0 (ring C attached to *t*Bu). Data for **(*R*,*S*)-3a**: $^1H$ NMR ($C_6D_6$, 25 °C) $\delta$ 0.35, 0.36, 0.50, 0.54 (s, 3 H, $SiCH_3$), 1.45, 1.50 (s, 9 H, $C(CH_3)_3$), 2.76, 2.79 (s, 3 H, $OCH_3$), 2.90−3.15 (m, 6 H, $NCH_2CH_2O$), 3.67 (m, 2 H, $NCH_2$), 6.08, 6.21 ("t", 1 H, ring H), 6.28 (m, 2 H, ring H), 6.43, 6.64 ("t", 1 H, ring H); $^1H$ NMR (THF-$d_8$, 21 °C) $\delta$ 0.21 (s, 3 H, $SiCH_3$), 0.22 (s, 6 H, $SiCH_3$), 0.25, (s, 3 H, $SiCH_3$), 1.25, 1.34 (s, 9 H, $C(CH_3)_3$), 3.17 (m, 2 H, $NCH_2CH_2O$), 3.41 (m, 1 H, $NCH_2CH_2O$), 3.48, 3.53 (s, 3 H, $OCH_3$), 3.51 (m, 3 H, $NCH_2CH_2O$), 3.67 (m, 2 H, $NCH_2CH_2O$), 5.68, 5.73, 5.97, 5.99, 6.12, 6.28 ("t", 1 H, ring H); $^{13}C$ NMR ($C_6D_6$, 25 °C) $\delta$ −3.5, −2.6, 3.2, 3.7 ($SiCH_3$), 32.4, 32.7 ($C(CH_3)_3$), 32.5, 33.2 ($C(CH_3)_3$), 51.2, 52.6 ($NCH_2$), 58.6, 58.7 ($OCH_3$), 79.1, 80.2 ($OCH_2$), 109.1, 110.0, 112.4, 112.8, 114.4, 119.4 (ring C), 113.2 (2 C, ring C), 142.4, 145.6 (ring C attached to *t*Bu). Anal. Calcd for $C_{28}H_{50}LiN_2O_2Si_2Y$: C, 56.17; H, 8.42; N, 4.68. Found: C, 55.47; H, 7.64; N, 5.67.

**Li[Y($\eta^5$:$\eta^1$-$C_5H_3tBuSiMe_2NCH_2CH_2NMe_2)_2$] (3b).** $YCl_3$ (391 mg, 2.00 mmol) and $Li_2(C_5H_3tBuSiMe_2NCH_2CH_2NMe_2)$ (1.11 g, 4.00 mmol) were combined in a flask, and precooled THF (30 mL) was added at −78 °C with stirring. The resulting mixture was allowed to warm to room temperature and stirred for 20 h. The solvent was removed in vacuo, and the crude product was extracted with 2 × 20 mL of toluene. LiCl was filtered off, and the clear solution was concentrated to 3 mL. After crystallization at −25 °C for 48 h, the mother liquor was decanted off and the product dried in vacuo to yield 725 mg (58%) of **3b** as colorless microcrystals. Data for **(*R*,*R*)-3b**: $^1H$ NMR ($C_6D_6$, 25 °C) $\delta$ 0.32, 0.54 (s, 6 H, $SiCH_3$), 1.42 (s, 18 H, $C(CH_3)_3$), 1.78 (br s, 12 H, $N(CH_3)_2$), 1.85, 2.59, 3.04, 3.19 (m, 2 H, $NCH_2CH_2N$), 6.19, 6.24, 6.54 ("t", 2 H, ring H); $^{13}C$ NMR ($C_6D_6$, 25 °C) $\delta$ −2.0, 2.9 ($SiCH_3$), 32.5 ($C(CH_3)_3$), 33.2 ($C(CH_3)_3$), 45.9 ($N(CH_3)_2$), 48.3 ($SiNCH_2$), 65.6 ($CH_2NMe_2$), 110.8 (ring C), 111.3 (ring C attached to $SiMe_2$), 113.0, 114.6 (ring C), 143.2 (ring C attached to *t*Bu). Data for **(*R*,*S*)-3b**: $^1H$ NMR ($C_6D_6$, 25 °C) $\delta$ 0.32, 0.33, 0.53, 0.55 (s, 3 H, $SiCH_3$), 1.43, 1.52 (s, 9 H, $C(CH_3)_3$), 1.78 (br s, 12 H, $N(CH_3)_2$), 1.9 (m, 2 H, $NCH_2CH_2N$), 2.4, 2.6 (m, 1 H, $NCH_2CH_2N$), 3.0−3.3 (m, 3 H, $NCH_2CH_2N$), 3.56 (m, 1 H, $NCH_2CH_2N$), 6.10 ("t", 1 H, ring H), 6.28 (m, 3 H, ring H), 6.38, 6.66 ("t", 1 H, ring H); $^{13}C$ NMR ($C_6D_6$, 25 °C) $\delta$ −2.3, −2.0, 3.0, 3.7 ($SiCH_3$), 32.4, 33.2 ($C(CH_3)_3$), 32.6, 32.9 ($C(CH_3)_3$), 45.9 ($N(CH_3)_2$), 48.2, 48.3 ($SiNCH_2$), 65.7, 65.8 ($CH_2NMe_2$), 109.6, 110.3, 110.8, 111.3, 111.4, 113.0, 114.3, 117.5 (ring C), 143.9, 145.9 (ring C attached to *t*Bu). Anal. Calcd for $C_{30}H_{56}LiN_4Si_2Y$: C, 57.67; H, 9.03; N, 8.97. Found: C, 55.79; H, 8.48; N, 8.82.

**Epimerization of (*R*,*S*)-3a.** A 5 mm NMR tube with a Teflon valve was charged with approximately 10 mg (17 $\mu$mol) of **(*R*,*S*)-3a** and 0.55 mL of THF-$d_8$. The sample was imme-

diateley inserted into the thermostated probe (±0.5 °C) of the Bruker DRX 400, and an initial ($t = 0$) $^1$H NMR spectrum was recorded. The time evolution of the integrals of the cyclopentadienyl protons at $\delta$ 5.68, 5.97, 5.99, 6.12, 6.28 (**(*R,S*)-3a**) and $\delta$ 5.93, 6.34 (**(*R,R*)-3a**) were monitored; the relative concentrations of the (*R,S*)- and (*R,R*)-diastereomer were determined from the relative areas of the integrals. The samples were allowed to reach equilibrium, and a final spectrum was recorded. The data were fit by linear least-squares analysis to the rate expression for the approach to equilibrium. The plot of $\ln\{(C_0 - C_{eq})/(C - C_{eq})\}$ ($C_0$, $C_{eq}$, and $C$ are the initial, at equilibrium, and at time $t$, respectively, percentage of (*R,S*)-diastereomer) versus time afforded ($k_1 + k_{-1}$) from the slope $a$.[26a] The forward rate constants ($k_1$) for the epimerization could be determined from the slope by the expression $k_1 = a \times (C_0 - C_{eq})/C_0$. The rate constants obtained at different temperatures were fit to the Eyring equation by linear least-squares analysis. $\Delta H^{\ddagger}$ and $\Delta S^{\ddagger}$ were obtained from the slope and the axial section.

**X-ray Crystal Structure Analysis of 1a·C$_6$D$_6$.** Crystal data for **1a·C$_6$D$_6$** are summarized in Table 1. The compound, obtained as colorless crystals by slow evaporation of benzene-$d_6$, crystallizes in the orthorhombic space group $P2_12_12_1$ as a mono(solvate). Data collection in the range $3° < \theta < 28°$ was performed using $\omega$ scans on an Enraf-Nonius CAD-4 diffractometer with graphite-monochromated Mo K$\alpha$ radiation. Friedel equivalent reflections in the chiral space group were measured. Data correction for Lorentz polarization and absorption (empirically using $\psi$ scans) was carried out using the program system MolEN.[49a] From 6739 measured reflections, all 6082 independent reflections were used and 394 parameters were refined by full-matrix least-squares against all $F_o^2$ data (SHELXL-93).[49b] The structure was solved using direct methods (SHELXS-86)[49c] and difference Fourier syntheses and refined with anisotropic thermal parameters for non-hydrogen atoms. Hydrogen atoms were calculated at their idealized positions. The refinement converged with R = 0.046, wR2 = 0.088 for all observed $F_0$ data; goodness of fit = 1.17.

**X-ray Crystal Structure Analysis of (*R,S*)-3a·$^1/_2$C$_6$H$_6$.** Crystal data for **(*R,S*)-3a·$^1/_2$C$_6$H$_6$** are summarized in Table 1. The compound, obtained as colorless prisms by slow evaporation of benzene, crystallizes in the triclinic space group $P\bar{1}$. Data collection in the range $3° < \theta < 28°$ was performed using $\omega$ scans on an Enraf-Nonius CAD-4 diffractometer with graphite-monochromated Mo K$\alpha$ radiation. Data correction for Lorentz polarization and absorption (empirically using $\psi$ scans) was carried out using the program system MolEN.[49a] From 9074 measured reflections, 8599 independent reflections were used and 364 parameters were refined by full-matrix least-squares against all $F_o^2$ data (SHELXL-93).[49b] The structure was solved using Patterson difference Fourier methods (SHELXS-86)[49c] and difference Fourier syntheses and refined with anisotropic thermal parameters for non-hydrogen atoms. Hydrogen atoms were calculated at their idealized positions. The refinement converged with R = 0.051, wR2 = 0.091 for all observed $F_0$ data; goodness of fit = 1.04.

**X-ray Crystal Structure Analysis of (*R,R*)-3b.** Crystal data for **(*R,R*)-3b** are summarized in Table 1. The compound, obtained as colorless prisms by slow evaporation of benzene, crystallizes in the monoclinic space group $C2/c$. Data collection in the range $3° < \theta < 30°$ was performed using $\omega$ scans on an Enraf-Nonius CAD-4 diffractometer with graphite-monochromated Mo K$\alpha$ radiation. Data correction for Lorentz polarization and absorption (empirically using $\psi$ scans) was carried out using the program system MolEN.[49a] From 13 894 measured reflections, 4359 independent reflections were used and 254 parameters were refined by full-matrix least-squares against all $F_o^2$ data (SHELXL-93).[49b] The structure was solved using direct methods (SHELXS-86)[49c] and difference Fourier syntheses and refined with anisotropic thermal parameters for non-hydrogen atoms. Hydrogen atoms were partially located and refined isotropically. The refinement converged with R = 0.039, wR2 = 0.073 for all observed $F_0$ data; goodness of fit = 1.12.

**Typical Polymerization of $\epsilon$-Caprolactone.** To a solution of the catalyst (25 $\mu$mol) in toluene (5 mL) or dichloromethane was added $\epsilon$-caprolactone using a syringe at room temperature with vigorous stirring. After 90 min, the polymerization was quenched by addition of methanol (4 mL) and the solvent was removed in vacuo. The polymer was redissolved in chloroform (5 mL) and precipitated into methanol (350 mL). The polymer was filtered and dried under vacuum.

**Oligomerization of $\epsilon$-Caprolactone.** In a 5 mm NMR tube with a Teflon valve the catalyst (10−30 mg) was dissolved in $C_6D_6$ (0.55 mL). $\epsilon$-Caprolactone (2−30 equiv) was placed at the upper end of the NMR tube to prevent early mixing. The NMR tube was closed and vigorously shaken.

**Acknowledgment.** Generous financial support by the Fonds der Chemischen Industrie, Volkswagen-Foundation, BASF AG (Kunststofflaboratorium), and the Bundesministerium für Bildung, Wissenschaft, Forschung und Technologie is gratefully acknowledged. K.C.H. thanks the Fonds der Chemischen Industrie for a doctoral scholarship. We thank Dr. B. Mathiasch and Mr. H. Kolshorn for obtaining various NMR spectroscopic data.

**Supporting Information Available:** Tables of all crystal data and refinement parameters, atomic parameters including hydrogen atoms, thermal parameters, and bond lengths and angles for **1a**, **2a**, **(*R,S*)-3a**, and **(*R,R*)-3b** and an ORTEP diagram of **2a** (35 pages). Ordering information is given on any current masthead page.

OM9705867



(49) (a) Fair, C. K. *MolEN, An Interactive Structure Solution Procedure*; Enraf-Nonius: Delft, The Netherlands, 1990. (b) Sheldrick, G. M. *SHELXL-93, Program for the Refinement of Crystal Structures*; University of Göttingen, Göttingen, Germany, 1993. (c) Sheldrick, G. M. *SHELXS-86, Program for the Solution of Crystal Structures*; University of Göttingen, Göttingen, Germany, 1986.